

NATIONAL PARK SERVICE
HISTORIC AMERICAN ENGINEERING RECORD

Addendum to
CONTOOCCOOK RAILROAD BRIDGE
HAER NO. NH-38

- Location: on the former Contoocook Valley (first Concord & Claremont, later Boston & Maine) Railroad line spanning over the Contoocook River, Contoocook village, Merrimack County, New Hampshire
- USGS Quadrangle: Hopkinton, New Hampshire (7.5-minute series)
- Year of construction: 1889
- Designer/Builder: Boston & Maine Railroad
- Structural type: Double-web Town lattice truss
- Present owner: New Hampshire Division of Historic Resources
- Present use: pedestrian bridge
- Significance: The Contoocook Railroad Bridge, built in 1889 on the former Concord and Claremont Railroad (acquired by Boston & Maine RR in 1887), is the oldest of the four surviving double-web Town lattice railroad bridges (Pier Bridge, Newport, NH, 1907; Wright's Bridge, Newport, NH, 1906; Fisher Bridge, Stowe, VT, 1908). It presents the clearest, most-original structure of its type, as the others incorporate significant structural modifications. The bridge was in use as a railroad bridge until 1962, survived a flood in 1936, a hurricane in 1938, and was moved off its foundations twice during its lifespan. Following its railroad service, it saw service as warehouse between 1962 and 1990.
- Authors: Researched and written by Dorottya Makay, August 2003
Supervised by Justin M. Spivey
- Project information: Phase II of the National Covered Bridges Recording Project was undertaken during the summer of 2003 by the Historic American Engineering Record (HAER), a long-range program to document historically significant engineering and industrial works in the United States. HAER (Eric DeLony, Chief) is part of the Historic American Buildings Survey/Historic American Engineering Record/Historic American Landscapes Survey/Cultural Resources Geographic Information Systems (E. Blaine Cliver, Chief), a division of the National Park Service, U.S. Department of the Interior. The Federal Highway Administration funded the project. The University of Vermont (Prof. Tom Visser, Director, Historic Preservation and Prof. Jean-Guy Beliveau, Chairman of Civil & Environmental Engineering) hosted the field team.
- The measured drawings, historical reports, engineering reports and photography were completed under the direction of Christopher Marston, Project Leader, Naomi

Hernandez, Summer Team Supervisor and Richard O'Connor, Senior Historian. The Burlington field team consisted of Field Supervisor Prof. Dr. Philip S. C. Caston (ICOMOS, Germany), Architects Vuong Dang (U. of Arkansas), William Dickinson (U. of Pennsylvania), Amy James (U. of Arkansas), Arnold Kreisel and Silvia Nadine Bauer (both ICOMOS, Germany), Michiko Tanaka (ICOMOS, Japan), and Doug Parker (U. of Oregon); and Historians Lola Bennett (Stow, MA) and Mark Brown (State College, PA). Engineering analyses were produced by Francesco Lanza (ICOMOS, Italy) working with Prof. John Ochsendorf (MIT); Dorottya Makay (ICOMOS, Romania) working with Justin M. Spivey (Robert Silman Assoc., NY); Megan Reese working with Prof. Dario Gasparini (both of Case Western Reserve U.); and Rachel Sangree working with Prof. Ben Schafer (both with Johns Hopkins U.). Large-format photography was produced by Jet Lowe, HAER Photographer.

Eduard J. Wojnowski, Administrator, Hopkinton, NH, provided on-site assistance.

INTRODUCTION

Wooden covered bridges represent an important section of the United States' built heritage. Over 800 timber covered bridges¹, representing 23 major types, still survive. Within the National Covered Bridges Recording Project—a three-year research program carried out by National Park Service's Historic American Engineering Record and sponsored by the Federal Highway Administration (FHWA)—the aim is to record one or more representative example of each major type through historical reports, architectural surveys, photographs and, in some cases, engineering analyses to identify the structural behavior of the trusses, as well as to promote their authentic preservation and rehabilitation.

Objectives of the study

This engineering report examines the Contoocook Railroad Bridge, the oldest of the four surviving double-web Town lattice bridges. Built in 1889, its structure is shown in Figure 1.²

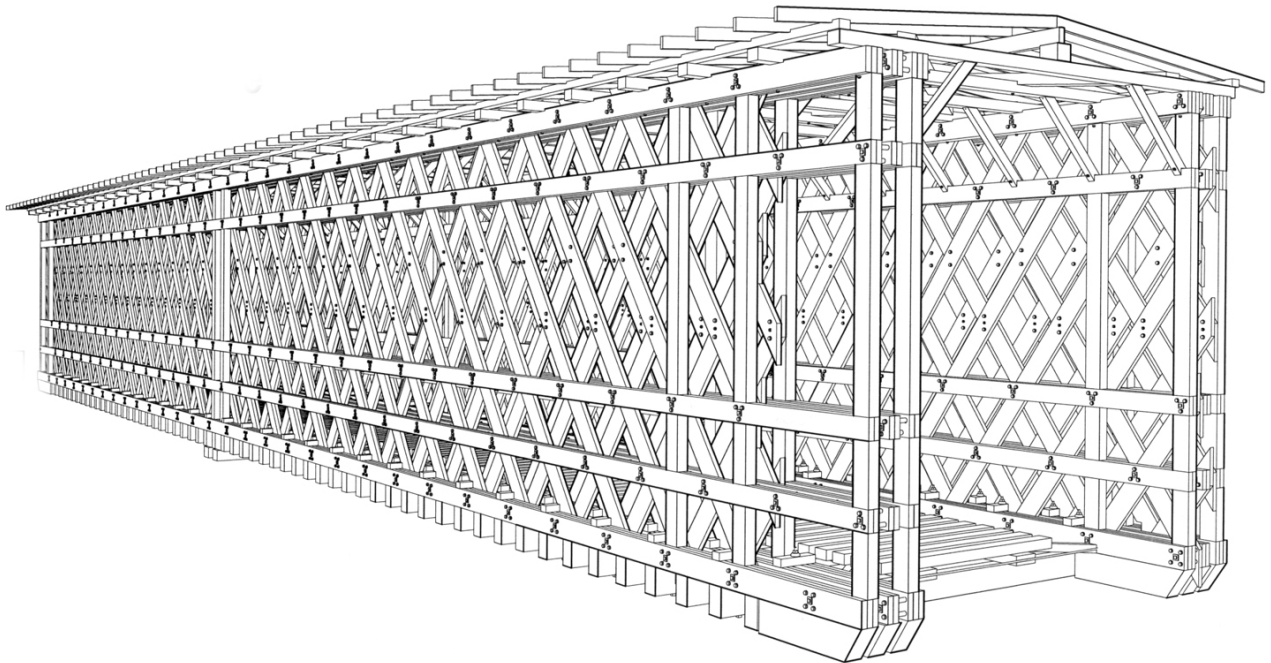


Figure 1. Structural configuration of the Contoocook Railroad Bridge – axonometric view³

Double-web Town lattice trusses represent the most developed version of these structures. With two lattice webs on each side, they were strong and stiff enough to carry railway live loads up to as much as Cooper's E50 loading specification. Though development of the lattice truss, first patented by Ithiel Town in 1820, was initially more empirical than engineered, they had become well-proportioned structures by the last half of the nineteenth century. Town lattice trusses, even double-web ones, were

¹ Philip C. Pierce, *Covered Bridge Manual*, draft, 2-15.

² Ibid.

³ Photographs and other illustration material were done by the author, unless otherwise noted. Architectural drawings were done by Amy James, HAER No. NH-38.

characterized by simple construction technology, relatively low material cost, and ease of erection using common wood construction techniques.

The principal objective of this study was to quantify the static behavior of one Double-web Town lattice trusses under both dead and live load conditions, and to investigate certain three-dimensional behaviors, including rotational and linear deformational stiffness of the various treenail joints, all to provide guidance for sustainable use, maintenance, and rehabilitation of this, and similar, structures.

To quantify the static behavior of the Contoocook Railroad Bridge, the following tasks were undertaken:

- identification of the timber species by the USDA’s Forest Products Laboratory
- identification of the geometry and load conditions—based on HAER team research
- identification of the treenailed joints’ rotational and linear deformational stiffness – based on HAER team research and local testing⁴
- calculation of joint stiffness through modeling and the use of existing former laboratory test results carried out by others⁵
- two- and three-dimensional finite element analyses of the structure under dead and live loads.

DOUBLE-WEB TOWN LATTICE TRUSSES AS RAILROAD BRIDGES

Historic context

Railroads required stiff, high-capacity bridges to withstand the large, dynamic live loads imposed by moving trains. Town’s first patent of simple diamond lattice webs with a recommended span-to-height ratio of 10:1 and a 45-degree angle for the lattice members would not have been stiff enough for railroad service.⁶ Timber was, however, considered a safe building material, since it gave evidence of distress long before failing, and it was chosen instead of iron in regions with abundant timber supply up to the beginning of the twentieth century. New England had numerous saw mills that could furnish lumber for Town lattice trusses, using wood from the area’s ample spruce forests, a specie that was ideal for truss structures. At the same time, iron production was limited in the region. These economic considerations had to be traded off against engineering challenges, too, especially as locomotive and train weights increased.⁷ Town’s double-web lattice, for which he received a patent in 1835 (Figure 2), provided the needed stiffness while retaining the lattice truss’s ease of construction. Together, these made wood a popular choice for New England bridges.

Although more technically advanced trusses were available to bridge designers by the time the Contoocook Bridge was built, and some critics disdained the Town truss, J. P. Snow, engineer of the Boston & Maine Railroad and builder of this bridge, felt otherwise.

“This style of bridge seems never have been developed to much extent outside of New England, and it is frequently referred to as peculiarly unscientific and wasteful of timber. It is however, the best of

⁴ Field load testing team was performed by Prof. Benjamin Shafer and Rachel Sangree, Johns Hopkins Univ.

⁵ Robert L. Brungaber and Leonard Morse-Fortier, *Wooden Peg Tests – Their Behavior and Capacities as Used in Town Lattice Trusses*, Vermont Department of Transportation, McFarland-Johnson consultant, Philip C. Pierce, project manager, tests performed at Massachusetts Institute of Technology, 1995.

⁶ J. G. James, *The Evolution of Wooden Bridge Trusses to 1850*, 1982.

⁷ “In 1895, a single-track bridge of 120-foot span cost about \$ 5,300 in iron, ... but only \$ 3,500 for a spruce lattice,” U. S. Department of the Interior, Historic American Engineering Record, No. NH-35, “Wright’s Bridge,” Washington, DC: Prints and Photographs Division, Library of Congress, 2002. “During the 1880s when Cooper first introduced his loading system, bridges were usually designed for loadings no greater than Cooper’s E20. By 1894 Cooper was recommending the use of his E40 loading as a standard...” William D. Middleton, *Landmarks on the Iron Road*, Bloomington, IN: Indiana University Press, 1999, 9.

the purely wooden bridges, and its present survival here and its economy over all other types disproves its wastefulness.”⁸

The most common and successful method of increasing a Town lattice truss’s capacity and stiffness was to build them with an initial upward bow, or camber. J. G. James believed that railroads could not tolerate camber,⁹ but Snow countered that designs with 1 inch of camber for each 25 feet of length presented no problems.¹⁰

In the same region, David Hazelton designed and built a number of double-web Town lattice railroad bridges, such as Warren Bridge, using triple lower and upper chords (Figure 3). Snow surely appreciated Hazelton’s activity, though he was a bridgewright instead of a trained engineer, but he questioned the concept, noting that, “... the tertiary chord has but little theoretical value, and judging by the amount that the joints are pulled they assist but little in carrying the chord strain.”¹¹

In comparison to the variety of improved double-web Town lattice structures, the Contoocook Bridge represents the “patent” well. Its analysis can provide a clear understanding of both the strengths and weaknesses of Town’s design and evaluate the necessity and ingenuity of the “enhancements” by Hazelton and Snow. A comparison between Figures 2, 3, and 4 reveal some of these changes.

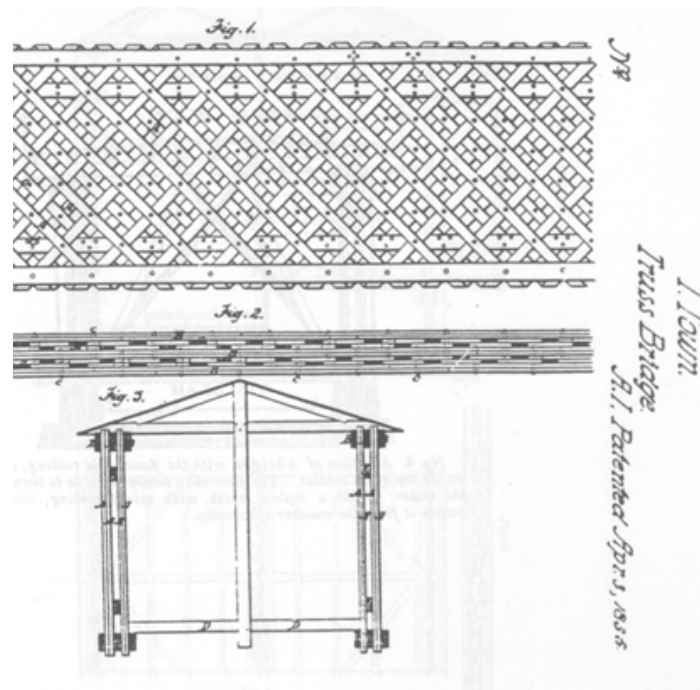


Figure 2. Town’s 1835 patent

⁸ J. P. Snow, “Wooden Bridge Construction on the Boston and Maine Railroad,” 1895, 31-43.

⁹ J. G. James, *The Evolution of Wooden Bridge Trusses to 1850*, 175.

¹⁰ J. P. Snow, “Wooden Bridge Construction on the Boston and Maine Railroad,” *Journal of Association of Engineering Society* XV, July 1895, 31-43, Also J. P. Snow, “A Recent All-wood Truss Railroad Bridge,” *The Engineering Record*. Vol. 60, No. 17, October 23, 1909, 456-457.

¹¹ J. P. Snow, “Wooden Bridge Construction on the Boston and Maine Railroad,” 1895, 36.

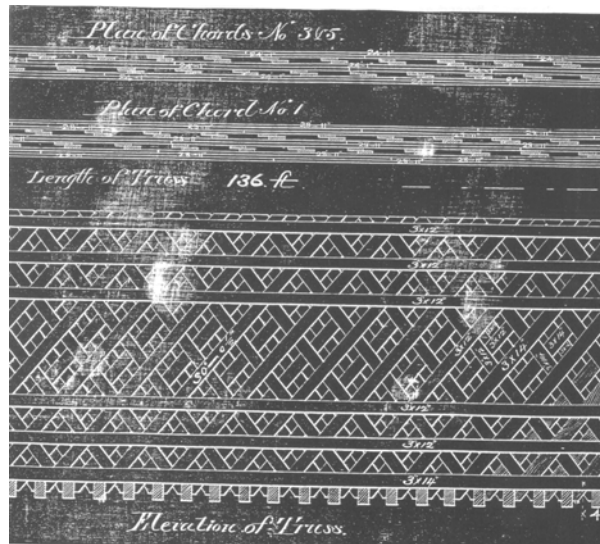


Figure 3. Hazelton's design for the Warren Bridge

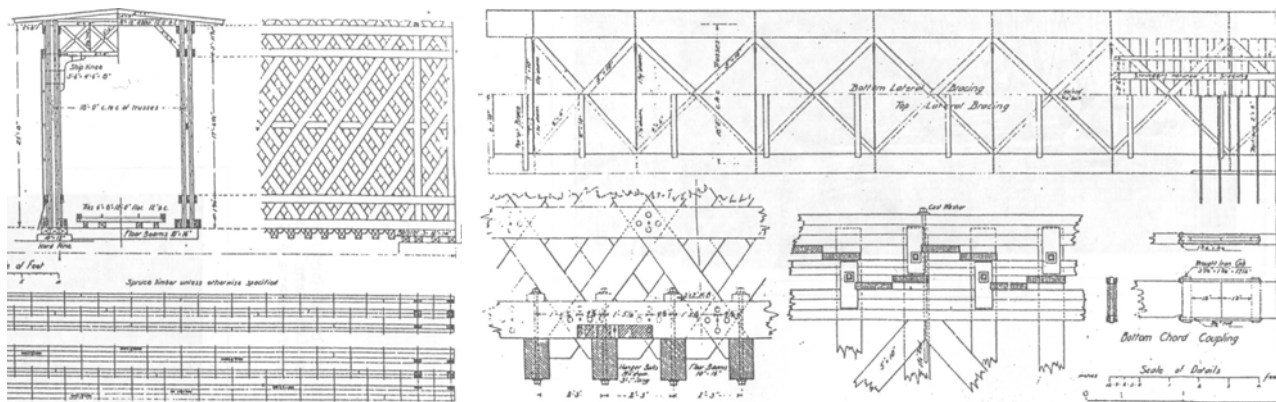


Figure 4. Snow's standard design

Classical simplified analysis of Town lattice structures

Due to their numerous interconnections, Town lattice trusses are statically indeterminate structures. As such, a thorough and accurate analysis of their behavior requires complex techniques that include individual-member-segment deformations in the stress calculations, or that deconstruct the truss into a series of Warren trusses. In the era before computers, most manual calculations used a simplified method known as equivalent beam analyses. In this method, the bending moment was broken into axial tension and compression couples with shear taken as axial forces by web members.

Historic load conditions

While a number of methods have been used over the years for determining the design loads for bridges, by far the most popular for railroad bridges has been the rating system developed by Theodore Cooper about five years before the Contoocook Bridge's construction. It was based on the driving axle weights of 2-8-0 steam locomotives, the most common type of the time. Designers reapportioned the axle weights of other locomotive wheel arrangements to an equivalent 2-8-0 to determine the appropriate Cooper rating. Snow provided an example of this for one 1895 bridge, where, "25,000 lb on each of three

axles [and a] 44 ft wheelbase for engine and tender”¹² corresponded to Cooper’s E10 rating, as shown in Figure 5. In Cooper’s scheme, the “E” indicates a locomotive, or “engine,” and the number specifies the weight on each driving axle in thousands of pounds. Note that the specification has two locomotives pulling the train.

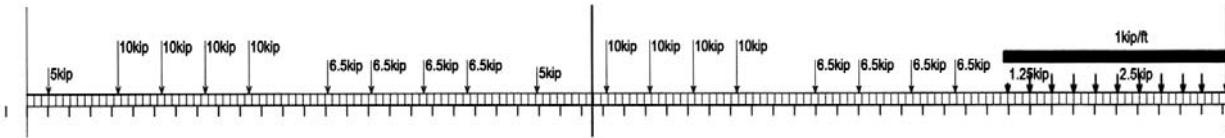


Figure 5. Cooper’s E10 load distribution¹³

Historic allowable stresses

While material properties and performance capabilities were only partially understood in the 1880s and 1890s, experience and what little theory there was gave designers useful information they could use with a reasonable degree of confidence. The most important parameter was the material’s allowable stress under different types of loads. Table 1 lists the values Snow used for one bridge he designed and built about 1909.

Table 1. Typical allowable stresses for eastern spruce¹⁴

| Allowable tension on net section | Allowable compression on gross section | Maximum flexure stress in floor beams | Maximum shear | Crushing pressure under washers | Maximum shear on oak trenails |
|----------------------------------|----------------------------------------|---------------------------------------|---------------|---------------------------------|-------------------------------|
| 1000 (800) psi | 700 (650) psi | 1200 psi | 100 (80) psi | 360 psi | 500 psi |

Though they began as empirical designs, double-web Town lattice trusses for railroad service constructions became well-designed structures that were designed using the most advanced structural analysis methods of the time. Taking a holistic approach to their design, builders were able to detail all the sub-structures and joints needed to construct a reliable bridge.

¹² “Talking about a 111½’ span bridge 17½’ deep apart of centers also giving the total weight of 100,000 board feet and 6000 lb iron,” in J. P. Snow, “Wooden Bridge Construction on the Boston and Maine Railroad,” 1895, 31-43.

¹³ William D. Middleton, *Landmarks on the Iron Road*, 1999.

¹⁴ Values of the table are from J. P. Snow, “A Recent All-wood Truss Railroad Bridge,” 1909, 456-457. Values in parentheses represent spruce design values given in J. P. Snow, “Wooden Bridge Construction on the Boston and Maine Railroad,” 1895, 31-43.

Trusses placed in mirror are generally considered to have good lateral stability. This was actually shown by the box-girder behavior of the Contoocook Bridge during floods and hurricanes that affected the bridge twice during its lifespan (Figure 7).¹⁵



Figure 7. Archive photograph of the Contoocook Railroad Bridge after being displaced by high water – New Hampshire Antiquarian Society, NH

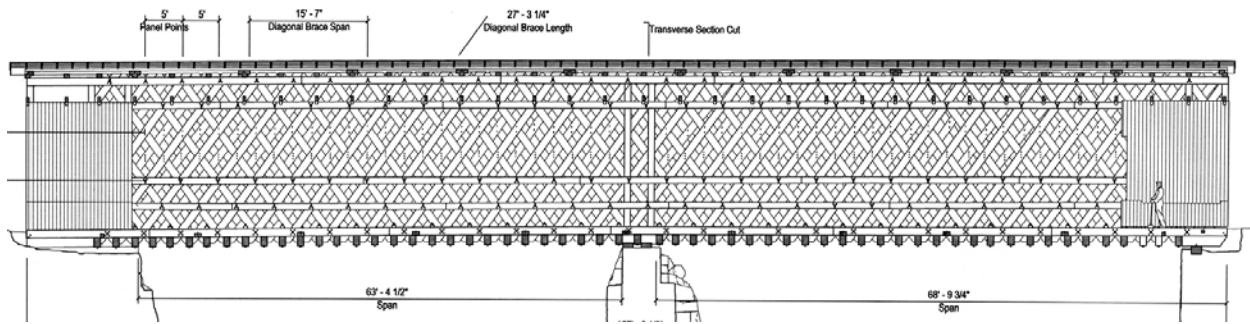


Figure 8. South truss, lateral view – HAER No. NH-38, “Contoocook Railroad Bridge,” 2003

Sub-structures

Both the floor system and track details are according to the common design of the time.¹⁶ Floor beams are suspended under the primary lower chord of the truss with 1¼ to 1½-inch iron rods with washers and timber blocks so that the floor beams are alternately loading the inner and the outer trusses.

¹⁵ C. Philip Pierce, *Covered Bridge Manual*, draft, 14-22. In a box girder, the entire structure, including the roof floor, and trusses, essentially form a stiff box and that acts as a unit to carry the vertical and horizontal loads.

¹⁶ The Plan of Standard Boston & Maine Railroad lattice truss supplied by J. P. Snow within his article in the *Journal of the Association of the Engineering Societies*, 1895 presents the same floor system solution, as it can be also found at the other two double Town lattice webs survived in the Sugar river-valley: Pier Bridge and Wright’s Bridge Newport, NH.

According to the architectural survey, 10 x 15-inch floor beams are spaced between 2 feet, 5 inches and 2 feet, 7 inches on centers. Figure 9 shows the floor system.

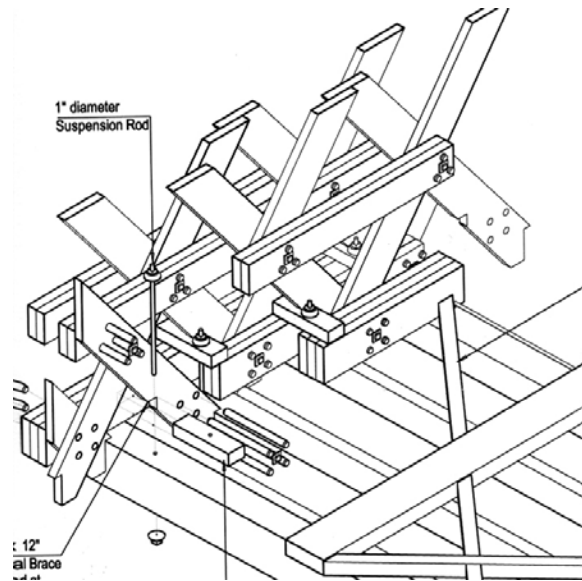


Figure 9. Floor system – HAER No. NH-38, “Contoocook Railroad Bridge,” 2003

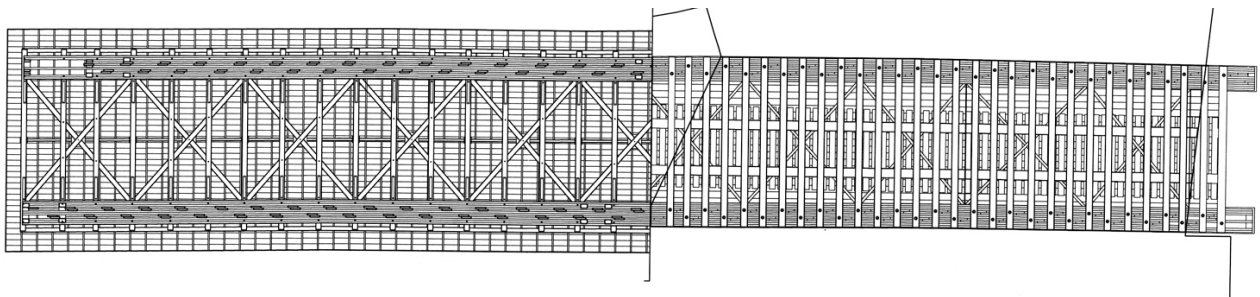


Figure 10. Roof (left) and floor (right) framing systems – HAER No. NH-38, “Contoocook Railroad Bridge,” 2003

The lower and upper laterals are modified Howe trusses, also according to standard design practice of the time, but the field inspection revealed a couple of unusual items. The lower diagonals are not continuous, but stopped and nailed to stringers, and the upper lateral braces have no iron ties, but rather timber ties at each lattice joint.

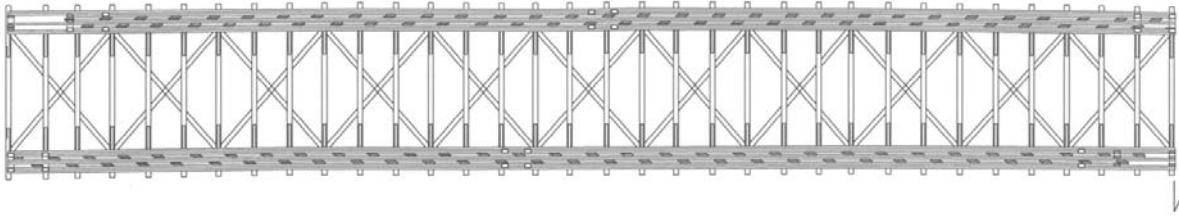


Figure 11. Upper lateral bracing system –HAER No. NH-38, “Contoocook Railroad Bridge,” 2003

The roof structure consists of principal and secondary rafters. Transverse bracing contributing to lateral stability is achieved through knee braces (Figure 13). The roof is covered with sheet metal at the present time, although it presumably was originally shingled, as was the common practice at the time.



Figure 12. Roof and knee brace detail

Characteristic features of Contoocook Railroad Bridge

Comparing the Contoocook Bridge to other surviving double-web Town lattice structures, as well as to standard designs published in the specialized literature, reveals a number of features that do not seem to be standard ones for the type, but appear to be details chosen by Snow to better suit this bridge to its site and function as a railroad bridge. These include:

- three lower chords instead of the patented and general two. Although it has only two sets of upper chords instead of Hazelton’s version of three lower and three upper chords.¹⁷
- seven lines of intersections. Snow’s published design includes nine rows of joint lines.
- a 2 foot, 6 inch floor-beam spacing, combined with 4 foot, 10³/₄-inch panel dimension. In Snow’s published design, the inter-axis displacement of floor beams is 2 feet, 3 inches, with a lattice panel dimension of 4 feet, 6 inches.
- A variety of treenail group patterns. Figure 13 shows the various patterns employed.

¹⁷ Snow also mentioned bridges built recently (before 1895) with three sets of chord, as well as those built by Hazelton, “... although they were built without engineering advice, they bear analysis well, with the possible exception on the bottom chords.”, J. P. Snow, “Wooden Bridge Construction on the Boston and Maine Railroad,” 1895, 36, 39.

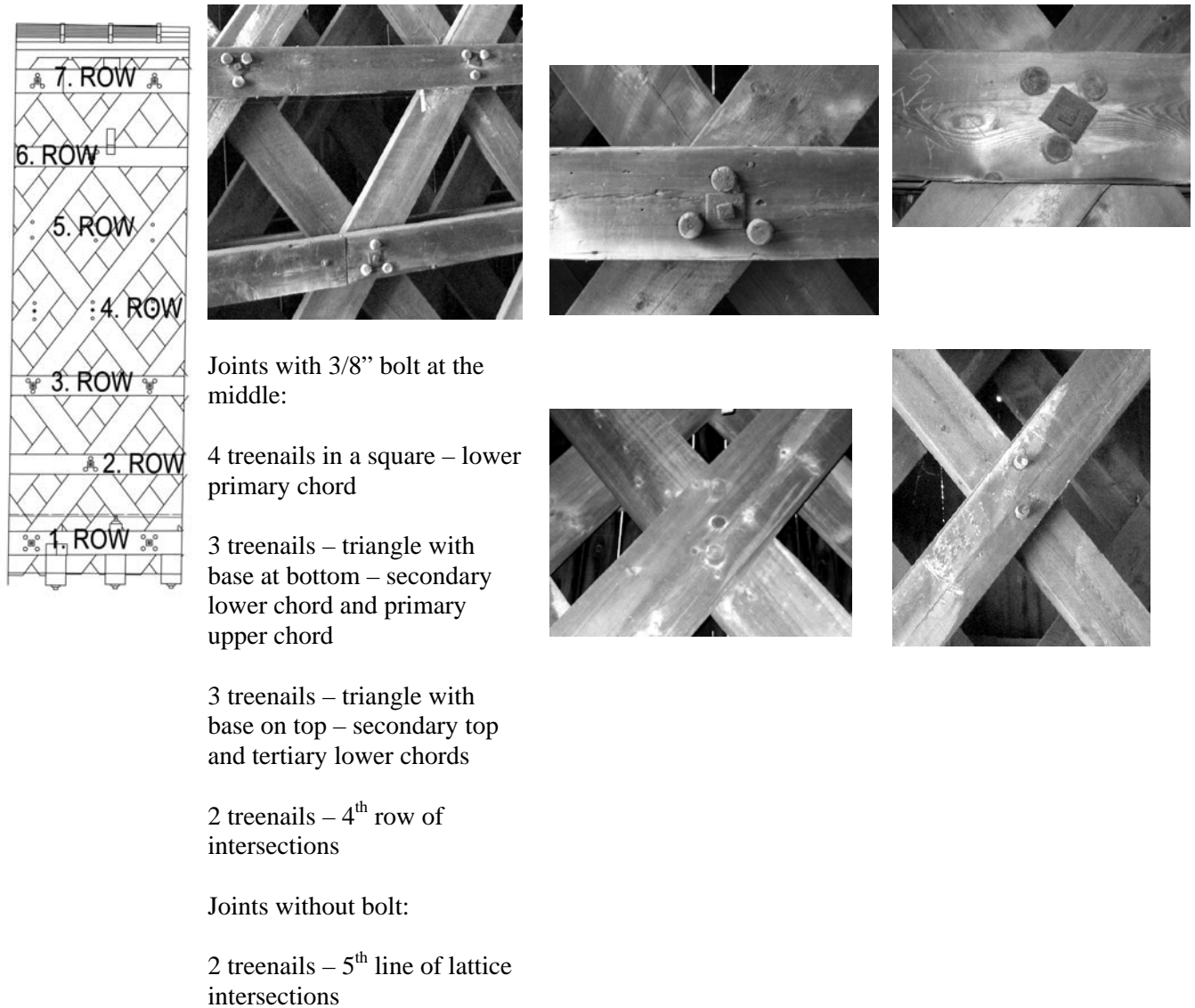


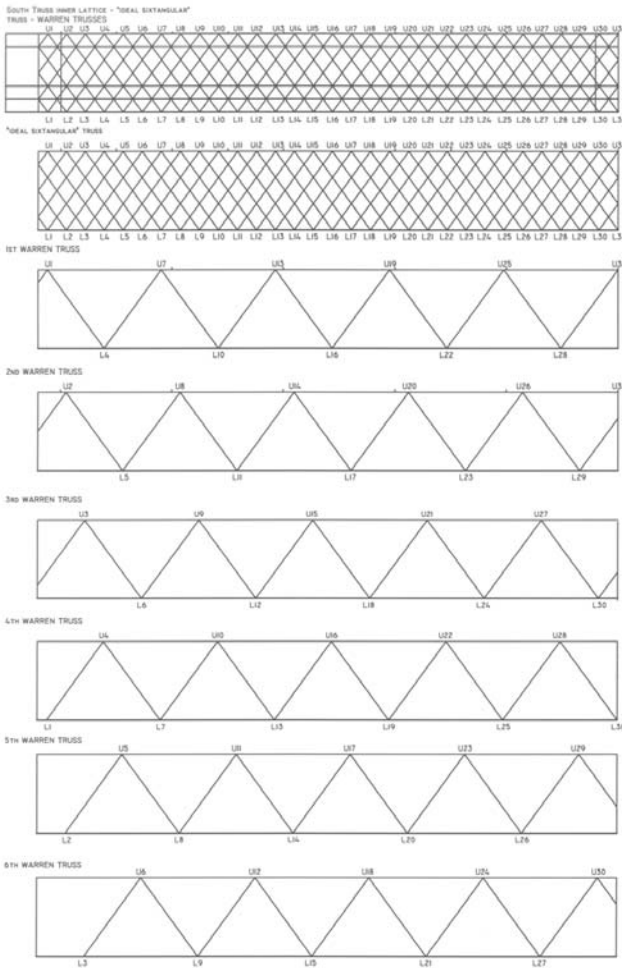
Figure 13. Different treenail-joint patterns used in the Contoocook Railroad Bridge

Structural determinacy and simplified (Warren) analysis

Town lattice trusses are statically indeterminate structures. For a single inner truss, the degree of indeterminacy (*N*) can be determined as follows:

$$N = m + r - 2j = 527 + 4 - (2 \times 227) = 77$$

where *m* = number of members, *r* = number of support reactions, and *j* = number of joints.



One single lattice is 77 times indeterminate. As there are connections between the two lattice webs as well, a double-web Town lattice truss would be more than twice as indeterminate as a simple lattice truss.

Theoretically, the Warren analysis makes these bridges computable by historic, hand calculations. Presumably, this, or an equivalent-beam analysis, was done for this bridge.

Figure 14. Deconstruction of a Town lattice truss into several Warren trusses to simplify the analysis

Present condition

Examination by the Forest Products Laboratory confirmed that the bridge was built using locally cut eastern spruce, a desirable specie for Town lattice truss construction.¹⁸ It has held up well. The bridge, being oversized from engineering point of view, is in very good condition. There is no sign of deflection at mid-span. The high degree of stiffness originally built into this bridge is no doubt a major reason for this good overall condition. There are some minor problems that do not have a significant influence on the bridge’s overall behavior. They can be grouped into two categories: problems related to the original design and construction, and problems related to later decay and repairs.

¹⁸ A copy of the wood identification test, performed by the Wood Anatomy Research Division, Forest Products Laboratory, Forest Service, USDA, is part of the field notes for this project.

Problems related to the original design and construction

These problems stem from the butt joints use to connect the chord members. Some of the planks are fixed with 3/8-inch bolts, but they are not adequate in size or number to carry the chord's tension loads. They may have been useful during assembly of the truss, presumably done while the timber was green (workability being better), to prevent independent lateral bending of the planks.¹⁹ Figure 15 shows one of these partially bolted splices. The structure contains symmetrically bolted (most frequent), half bolted, and simple butt joints with no bolts.

A number of splices are placed in such a way that they interfere with the lattice-chord joints, making the joint weaker. One of these is shown in Figure 16. Although the splices have been surveyed and these interferences noted, they were not introduced into the 3D model except as reduced member cross-sections.

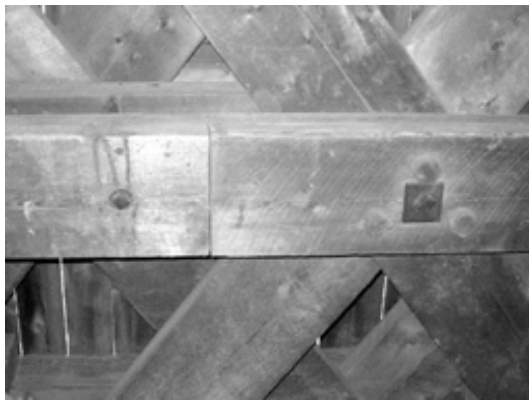


Figure 15. Partially bolted splice



Figure 16. Splice interfering with a chord-lattice joint

Problems related to later decay and repairs

A number of lattice webs present longitudinal (shear or shrinkage) cracks that were reinforced by the addition of iron clamps to hold the two parts firmly together (Figure 16). On the level of the secondary lower chord, there is a similar, but probably older, reinforcement intervention. Here there are clamps formed both by timber and iron elements to reinforce a cracked chord member (Figure 17). This intervention might be of the same age as the bridge.

¹⁹ Snow's report is actually saying the same also about the 3/4" bolts for lattice joints, but taking into consideration also 800 pound in transmission of tension forces; J. P. Snow, "Wooden Bridge Construction on the Boston and Maine Railroad", 1895., 31-43.



Figure 17. Lattice reinforcement using an iron clamp



Figure 18. Secondary lower chord reinforcement with clamps

The northern truss has evidence of more intervention. There are several of the iron clamps just described, but major decay is marked by the following interventions as well:

- extra hanger beams of 12 feet x 11¾ inches square were inserted at both abutments (floor beams 56, 57, and 58 were hung at the western side to the extra hanger beam, being supported by the abutment and beam 56). The same system was repeated at East side for floor beams 1, 2, and 3.
- the same hanger system was used at the pier for floor beams 27, 28, and 29, which were suspended from the hanger beam that is supported by beams 26 and 30.

Structural analysis of the Contoocook Railroad Bridge

The overall beam behavior of Town lattice bridges generally has been exhaustively detailed in the engineering report addendum to HAER's report on the Brown Bridge, therefore this analysis focused on other questions about the Town lattice truss—especially double-web lattice structures.²⁰ The primary investigative process involved mathematical modeling using SAP2000 linear finite element analysis software, supplemented by Axis VM7 software.

The questions to be resolved, along with descriptions of the investigative model variants, are as follows:

1. How does the existence of splices influence the overall behavior of the structure (stiffness, mid-span deflection under dead load)?

Two-dimensional models created to identify the differences with the different applicable combinations of rigid (infinite stiff joints) and pinned (rotationally flexible) joints in the primary lower and upper chords and lattice intersections as follows:

- Var 1. 2D inner lattice, stiff joints, full section of chords.
- Var 2. 2D inner lattice, stiff joints, reduced section of chords (50% for chords made up of two elements, and 33% where chord is made up of three elements).
- Var 3. 2D inner lattice, pinned joints at lattice ends, reduced section of chords.
- Var 4. 2D inner lattice, pinned joints at lattice ends, reduced section of chords, single span (No central pier, but the same load conditions).

²⁰ HAER No. VT-28, "Brown Bridge", 2002.

2. Would it have been better, i.e., more economical, to develop a proper joint for tension transmission instead of adding the tertiary lower chord?

Var 5. 2D inner lattice, pinned joints at lattice ends, reduced section of chords, tertiary chord missing (to identify the efficiency of introducing the tertiary lower chord versus tension joints at the splices).

3. Would a single-span bridge have been preferable to the two-span bridge actually built?

Some of the historic evidence mentions the Contoocook Railroad Bridge as a 157-foot single-span structure, so the differences between the actual double-span bridge and an equivalent single-span version have been compared.

4. Were the designer's choices for web member angle, number of intersections, and truss proportions the optimum ones?
5. How much did doubling the lattice truss affect its overall stiffness?

This involved the construction of the following two-dimensional and three-dimensional models:

Var 6. 2D both lattice webs, pinned joints at lattice ends, reduced section of chords.

Var 7. 3D inner lattice webs, mathematically modeled joint stiffness, both total and reduced sections of chords.

Var 8. 3D both lattice webs, mathematically modeled joint stiffness, both total and reduced sections of chords.

Historic structures, even if they are engineered or semi-engineered ones, are not (or at least not perfectly) regular, so it was necessary to decide whether to model the truss as ideal, with parallel lines and perfect joints, or as a deformed structure with all of its irregularities.

Since the differences/deformations (see Figure 19) are small enough to be irrelevant to the overall behavior from a structural point of view, the models were constructed as ideal structures to simplify the calculations. To introduce real joint stiffness, a 3D model of one double-web lattice truss was created (Figure 20).

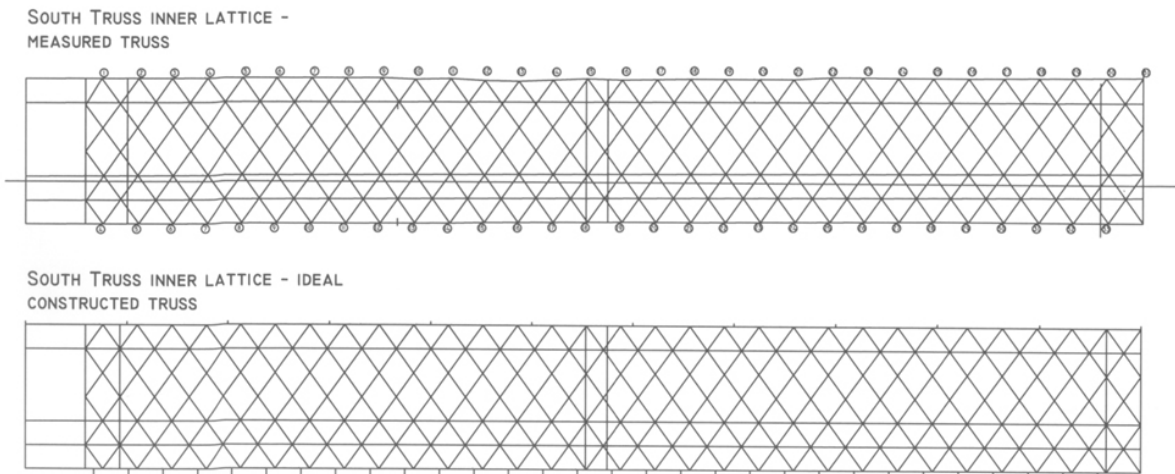


Figure 19. Comparative model of the real (measured) and ideal structure, as used for present report

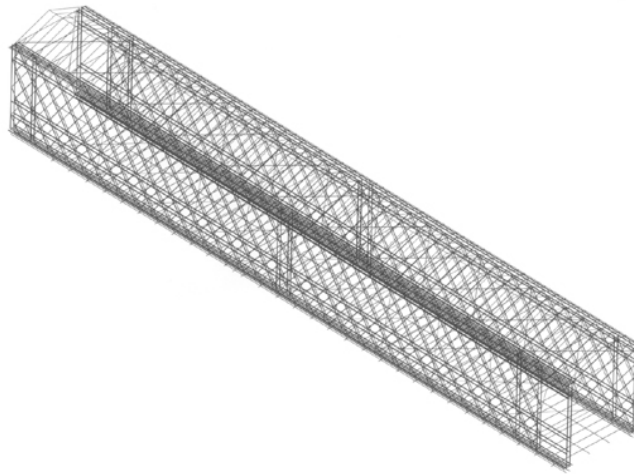


Figure 20. 3D model of the bridge

The bridge was built using eastern spruce, which has the mechanical properties listed in Table 1.

Table 1. Mechanical properties of eastern spruce

| | kip in | lb ft |
|------------------------|----------------------|----------------------|
| Mass per unit volume | 4.40E ⁻⁰⁸ | 0.9133 |
| Weight per unit volume | 1.70E ⁻⁰⁵ | 29.3976 |
| Modulus of elasticity | 1340.277 | 1.93E ⁺⁰⁸ |
| Poisson ratio | 0.372 | 0.372 |

Table 2 lists the section characteristics for both full and reduced cross sections of the chords.

Table 2. Section characteristics for chords

| Var 1. Full section | | | | | | Var 2. Reduced sections | | | | | |
|---------------------|------------------------------------------------------------------|-------|-------|-----------------|-----------------|-------------------------|---------------------------------------------------------------|-------|-------|-----------------|-----------------|
| No. | Name of section | Width | Depth | Area | <i>I</i> | No. | Name of section | Width | Depth | Area | <i>I</i> |
| | | in | in | in ² | in ⁴ | | | in | in | in ² | in ⁴ |
| 1 | Chord total: main chord lower + upper | 11 | 11.75 | 129.25 | 1487.048 | 1 | Chord total: main chord lower + upper | 8.25 | 11.75 | 96.9375 | 1115.286 |
| 2 | Second. chords total: secondary chords lower + upper | 8.25 | 9.75 | 80.4375 | 637.2158 | 2 | Second. chords total: secondary chords lower + upper | 5.5 | 9.75 | 53.625 | 424.8105 |
| 3 | Lattice | 2.75 | 11.75 | 32.3125 | 371.762 | 3 | Lattice | 2.75 | 11.75 | 32.3125 | 371.762 |
| 4 | Stud (post) | 5.5 | 9.75 | 53.625 | 424.8105 | 4 | Stud (post) | 5.5 | 9.75 | 53.625 | 424.8105 |

Table 4. Equivalent inertia and load needed to achieve 1/8-inch deflection at mid-span of 70-foot single- span equivalent beam

| No. | Neutral axes | Equivalent inertia (I) | Uniform load (plf) | Concentrated load (kip) |
|-----|-----------------|------------------------------|--------------------|-------------------------|
| 1. | $y = 110.12$ in | 9154322.54 in ⁴ | 19.71 | 124.178 |
| 2. | $y = 109.67$ in | 5456137.48 in ⁴ | 11.75 | 74.012 |

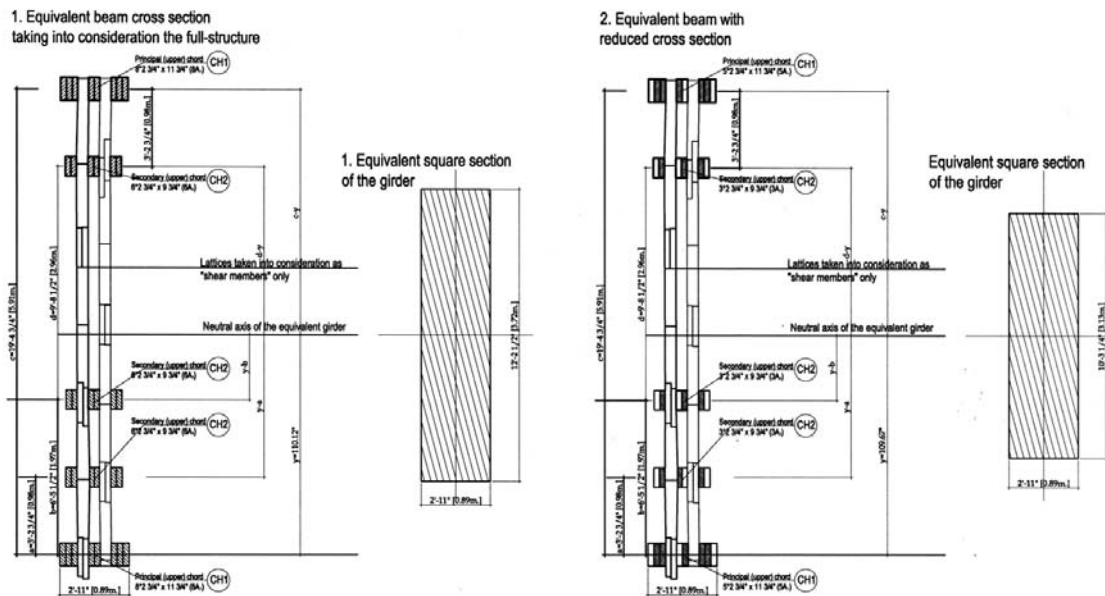


Figure 21. Equivalent beam sections – inertia calculation

These results show that the stiffness of condition 2 (spliced chords), measured in concentrated force applied at mid-span to achieve 1/8” deflection, is 40.4 percent less than that of condition 1 (continuous chords). But even with the condition 2, a 74-kip load would be required to achieve a 1/8” (the minimum measurable) deflection. This led the team to cancel the idea of load testing the bridge to measure overall deflection.²¹

As some of historic evidences mention Contoocook Railroad Bridge with a single 157-foot span, the merits of this hypothesis were considered throughout this report. Even with such a span, the stiffness (measured in middle span deflection) of the double-web Contoocook Bridge is three times greater than that of a single-web Town lattice bridge commonly used in roadway service.²²

²¹ U.S. Department of Interior American Engineering Record, HAER No. VT-30, “Taftsville Bridge”, 2003, (Prints and Photographs Division, Library of Congress Washington, D.C.) – field load testing was carried with 11.8kip, appreciatively 6 time less than the one needed at Contoocook;

²² U.S. Department of Interior American Engineering Record, HAER No. NH-33, “Bath-Haverhill Bridge”, 2003, (Prints and Photographs Division, Library of Congress Washington, D.C.);

Comparison of two-dimension finite element models under dead and live load conditions

For the inner lattice analysis (Var 1, Var 2, Var 3, and Var 4), a comparison of the trusses' behaviors was made on the basis of analyzing the following characteristics:

- deflection at mid-span under various load conditions.
- maximum axial force (tension and compression) in the characteristic members (L-1 = principal lower chord; L-2 = secondary lower chord; L-3 = tertiary lower chord; U-1 = principal upper chord; U-2 = secondary upper chord; D = lattice diagonal).
- maximum bending moment in the same elements.

The results of the finite element analysis are summarized in Tables 4 through 8.

Table 4. Mid-span deflection comparison data

| No | Value to compare | Load case | Var 1. – Stiff joint + full chord | Var 2. – Stiff joint + reduced chord | Var 3. – Pin joints + reduced chord | Var 4. – Pin joints + reduced chord single span |
|-----|--------------------------|--------------------------------------|-----------------------------------|--------------------------------------|-------------------------------------|-------------------------------------------------|
| 1.1 | Mid-span deflection (in) | dead load | -0.071271 | -0.072544 | -0.073227 | -0.960914 |
| 1.2 | | concentrated load at mid span | -0.537686 | -0.585876 | -0.592842 | -2.968619 |
| 1.3 | | Live load Cooper's E20 | -0.140883 | -0.152804 | -0.154254 | -2.556176 |
| 1.4 | | reduced concentrated | -0.320877 | -0.349636 | -0.353793 | -1.771595 |
| 1.5 | | Combination dead load + Cooper's E20 | -0.212154 | -0.225348 | -0.227481 | -3.51709 |

These data are the values of mid-span deflection. A comparison to Var 2, which was considered to be the base (control) value, indicated the following:

- The introduction of pinned joints at lattice ends reduces stiffness only 1 percent.
- The increase of stiffness, measured in mid-span deflection, by having continuous chords (Var 1) is less than 10 percent, about one-fifth of the 50 percent estimated with the equivalent beam analysis.
- The deflection increased 4 to 15 times when the span was doubled, with less increase for a concentrated load (influenced by span on the 3rd), and the greatest increase for distributed loads (depending on span at the 4th).

Table 5. Change of stiffness

| Load case | Stiffness increase % Var 1/2. | Stiffness increase % Var 3/2. | Deflection increase % Var 3/4. | Deflection/span ratio (71') Var 3 | Deflection/span ratio (144') Var 4 |
|---------------------------------------|-------------------------------|-------------------------------|--------------------------------|-----------------------------------|------------------------------------|
| Dead load | 1.74 | 0.93 | 1212.24 | 1/11500 | 1/1750 |
| Concentrated load at mid-span | 8.13 | 1.18 | 400.74 | 1/1430 | 1/560 |
| Live load Cooper's E20 | 7.73 | 0.94 | 1557.12 | 1/5500 | 1/657 |
| Reduced concentrated load at mid-span | 8.13 | 1.17 | 400.74 | 1/2400 | 1/948 |

| | | | | | |
|--------------------------------------|------|------|---------|--------|-------|
| Combination dead load + Cooper's E20 | 5.80 | 0.94 | 1446.10 | 1/3730 | 1/470 |
|--------------------------------------|------|------|---------|--------|-------|

The deflection-to-span ratios are very low, but the inner joints were modeled as stiff joints, which increased the calculated stiffness.

Table 6. Axial forces in chord members

| No | Value to compare | Load case | Stiff joint + full chord | Stiff joint + reduced chord | Pin joints + reduced chord | Pin joints + reduced chord single span | Change 1/2 | Change 2/3 | Change 4/3 |
|-----|-----------------------|---------------------------------------|--------------------------|-----------------------------|----------------------------|----------------------------------------|------------|------------|------------|
| 2.1 | Maximum tension (kip) | Dead load | 8.416 | 8.468 | 8.33 | – | 0.61 | -1.66 | |
| 2.2 | PRIMARY UPPER CHORD | Concentrated load at mid-span | 43.108 | 46.94 | 46.517 | – | 8.16 | -0.91 | |
| 2.3 | member id 465 | Live load Cooper's E20 | 17.768 | 19.431 | 19.236 | – | 8.56 | -1.01 | |
| 2.4 | | Reduced concentrated load at mid-span | 25.726 | 28.012 | 27.76 | – | 8.16 | -0.91 | |
| 2.5 | | Combination dead load + Cooper's E20 | 26.184 | 27.899 | 27.566 | – | 6.15 | -1.21 | |
| 3.1 | Maximum tension (kip) | Dead load | 4.727 | 4.21 | 4.207 | 28.85 | -12.28 | -0.07 | 585.76 |
| 3.2 | PRIMARY LOWER CHORD | Concentrated load at mid-span | 39.02 | 37.346 | 34.903 | 99.929 | -4.48 | -7.00 | 186.30 |
| 3.3 | member id 257/472 | Live load Cooper's E20 | 11.548 | 10.973 | 11.026 | 76.184 | -5.24 | 0.48 | 590.95 |
| 3.4 | | Reduced concentrated load at mid-span | 23.286 | 22.287 | 20.829 | 59.635 | -4.48 | -7.00 | 186.31 |
| 3.5 | | Combination dead load + Cooper's E20 | 16.275 | 15.183 | 15.234 | 105.034 | -7.19 | 0.33 | 589.47 |
| 4.1 | Maximum tension (kip) | Dead load | 1.322 | 1.147 | 1.167 | 8.769 | -15.26 | 1.71 | 651.41 |
| 4.2 | SECONDARY LOWER CHORD | Concentrated load at mid-span | -12.165 | -11.604 | -11.752 | -3.742 | -4.83 | 1.26 | -68.16 |
| 4.3 | member id 236/444 | Live load Cooper's E20 | 4.397 | 4.216 | 4.317 | 22.38 | -4.29 | 2.34 | 418.42 |
| 4.4 | MS | Reduced concentrated load at mid-span | -7.26 | -6.925 | -7.013 | -2.233 | -4.84 | 1.25 | -68.16 |
| 4.5 | | Combination dead load + Cooper's E20 | 5.719 | 5.363 | 5.484 | 31.084 | -6.64 | 2.21 | 466.81 |
| 5.1 | Maximum tension (kip) | Dead load | 2.681 | 2.224 | 1.929 | – | -20.55 | -15.29 | |
| 5.2 | SECONDARY LOWER CHORD | Concentrated load at mid-span | 6.691 | 5.451 | 4.311 | – | -22.75 | -26.44 | |
| 5.3 | member id 473 | Live load Cooper's E20 | 6.656 | 6.003 | 5.276 | – | -10.88 | -13.78 | |
| 5.4 | MP | Reduced concentrated load at mid-span | 3.993 | 3.253 | 2.573 | – | -22.75 | -26.43 | |
| 5.5 | | Combination dead load + Cooper's E20 | 9.337 | 8.227 | 7.205 | – | -13.49 | -14.18 | |
| 6.1 | Maximum tension (kip) | Dead load | 3.556 | 2.952 | 2.974 | 1.651 | -20.46 | 0.74 | -44.49 |
| 6.2 | THIRD LOWER CHORD | Concentrated load at mid-span | 12.089 | 10.2 | 10.262 | -16.973 | -18.52 | 0.60 | - |
| 6.3 | member id 475 | Live load Cooper's E20 | 8.239 | 7.364 | 7.404 | 1.704 | -11.88 | 0.54 | -76.99 |
| 6.4 | MP | Reduced concentrated load at mid-span | 7.215 | 6.087 | 6.124 | -10.129 | -18.53 | 0.60 | - |

| | | | | | | | | | |
|-----|---------------------------|---------------------------------------|---------|---------|---------|----------|--------|------|--------|
| 6.5 | | Combination dead load + Cooper's E20 | 11.795 | 10.316 | 10.379 | 3.355 | -14.34 | 0.61 | -67.68 |
| 7.1 | Maximum compression (kip) | Dead load | -8.086 | -7.45 | -7.475 | -48.505 | -8.54 | 0.33 | 548.90 |
| 7.2 | PRIMARY UPPER CHORD | Concentrated load at mid-span | -54.639 | -54.826 | -55.038 | -165.457 | 0.34 | 0.39 | 200.62 |
| 7.3 | member id 225/465 | Live load Cooper's E20 | -24.419 | -24.424 | -24.497 | -130.831 | 0.02 | 0.30 | 434.07 |
| 7.4 | MS | Reduced concentrated load at mid-span | -32.607 | -32.719 | -32.845 | -98.74 | 0.34 | 0.38 | 200.62 |
| 7.5 | | Combination dead load + Cooper's E20 | -32.505 | -31.874 | -31.972 | -179.335 | -1.98 | 0.31 | 460.91 |
| 8.1 | Maximum compression (kip) | Dead load | -3.314 | -2.8 | -2.833 | -19.486 | -18.36 | 1.16 | 587.82 |
| 8.2 | SECONDARY UPPER CHORD | Concentrated load at mid-span | -24.014 | -22.182 | -22.477 | -74.168 | -8.26 | 1.31 | 229.97 |
| 8.3 | member id 206/471 | Live load Cooper's E20 | -10.738 | -9.815 | -9.932 | -53.382 | -9.40 | 1.18 | 437.47 |
| 8.4 | MS | Reduced concentrated load at mid-span | -14.331 | -13.238 | -13.414 | -44.261 | -8.26 | 1.31 | 229.96 |
| 8.5 | | Combination dead load + Cooper's E20 | -14.053 | -12.615 | -12.765 | -72.868 | -11.40 | 1.18 | 470.84 |

Note: MS = mid-span area, MP = middle pier area.

Secondary upper chord tension values are not included in the comparative results table.

Table 7. Axial forces in lattice members

| No | Value to compare | Load case | Stiff joint + full chord | Stiff joint + reduced chord | Pin joints + reduced chord | Pin joints + reduced chord single span | Change 1/2 | Change 2/3 | Change 4/3 |
|------|---------------------------|---------------------------------------|--------------------------|-----------------------------|----------------------------|----------------------------------------|------------|------------|------------|
| 9.1 | Maximum tension (kip) | Dead load | 4.457 | 4.096 | 4.346 | 7.442 | -8.81 | 5.75 | 71.24 |
| 9.2 | in lattice member | Concentrated load at mid-span | 14.572 | 14.478 | 15.417 | 12.521 | -0.65 | 6.09 | -18.78 |
| 9.3 | MP | Live load Cooper's E20 | 13.636 | 13.509 | 14.472 | 19.263 | -0.94 | 6.65 | 33.11 |
| 9.4 | 515/902 | Reduced concentrated load at mid-span | 8.696 | 8.64 | 9.201 | 7.472 | -0.65 | 6.10 | -18.79 |
| 9.5 | | Combination dead load + Cooper's E20 | 18.093 | 17.605 | 18.819 | 26.705 | -2.77 | 6.45 | 41.90 |
| 10.1 | Maximum tension (kip) | Dead load | 1.386 | 1.349 | 1.377 | 0.656 | -2.74 | 2.03 | -52.36 |
| 10.2 | in lattice member | Concentrated load at mid-span | 65.509 | 53.658 | 56.272 | 65.509 | -22.09 | 4.65 | 16.41 |
| 10.3 | MS | Live load Cooper's E20 | 4.358 | 4.471 | 4.434 | 5.92 | 2.53 | -0.83 | 33.51 |
| 10.4 | 251/460 | Reduced concentrated load at mid-span | 31.692 | 32.022 | 33.582 | 39.094 | 1.03 | 4.65 | 16.41 |
| 10.5 | | Combination dead load + Cooper's E20 | 5.744 | 5.82 | 5.811 | 6.576 | 1.31 | -0.15 | 13.16 |
| 11.1 | Maximum compression (kip) | Dead load | -8.552 | -8.132 | -8.399 | -13.027 | -5.16 | 3.18 | 55.10 |
| 11.2 | in lattice member | Concentrated load at mid-span | -30.744 | -31.794 | -32.807 | -22.653 | 3.30 | 3.09 | -30.95 |

| | | | | | | | | | |
|------|---------------------------|---------------------------------------|---------|---------|---------|---------|--------|-------|--------|
| 11.3 | MP | Live load Cooper's E20 | -19.541 | -20.166 | -20.704 | -30.108 | 3.10 | 2.60 | 45.42 |
| 11.4 | 459/924 | Reduced concentrated load at mid-span | -18.347 | -18.974 | -19.578 | -13.519 | 3.30 | 3.09 | -30.95 |
| 11.5 | | Combination dead load + Cooper's E20 | -28.115 | -28.319 | -29.124 | -43.113 | 0.72 | 2.76 | 48.03 |
| 12.1 | Maximum compression (kip) | Dead load | -0.267 | -0.283 | -0.318 | 0.031 | 5.65 | 11.01 | 109.75 |
| 12.2 | in lattice member | Concentrated load at mid-span | -19.833 | -19.902 | -23.142 | -13.603 | 0.35 | 14.00 | -41.22 |
| 12.3 | MS | Live load Cooper's E20 | 1.594 | 1.477 | 1.592 | 2.662 | -7.92 | 7.22 | 67.21 |
| 12.4 | 278/515 | Reduced concentrated load at mid-span | -11.836 | -11.877 | -13.811 | -8.118 | 0.35 | 14.00 | -41.22 |
| 12.5 | | Combination dead load + Cooper's E20 | 1.328 | 1.194 | 1.274 | 2.693 | -11.22 | 6.28 | 111.38 |

The first two models with only stiff joints contributed to bending moment concentrations on abutment studs and chords, but this was unrealistic, and as such was not considered further. Even versions with pinned joints at the lattice ends introduce a bending moment concentration at single support points. This should be different in reality, due to more support points between the abutment and bolster beam. "Bolster beam," as used here, represents a distributed line of support for the bridge that could not be modeled with the software used. Therefore, large negative values of support bending moments were not included in the table below.

Table 8. Bending moment comparison table

| No | Value to compare | Load case | Stiff joint + full chord | Stiff joint + reduced chord | Pin joints + reduced chord | Pin joints + reduced chord single span | Change 1/2 % | Change 2/3 % | Change 4/3 % |
|------|----------------------------------|---------------------------------------|--------------------------|-----------------------------|----------------------------|----------------------------------------|--------------|--------------|--------------|
| 13.1 | Mid-span bending moment (kip-ft) | Dead load | 0.735 | 0.5352 | 0.2963 | 1.6458 | -37.26 | -80.63 | 455.45 |
| 13.2 | PRIMARY BOTTOM CHORD | Concentrated load at mid-span | 3.348 | 2.973 | 1.8037 | 3.2495 | -12.62 | -64.83 | 80.16 |
| 13.3 | MP | Live load Cooper's E20 | 5.471 | 5.3106 | 5.1784 | 4.4966 | -3.02 | -2.55 | -13.17 |
| 13.4 | 440/58 | Reduced concentrated load at mid-span | 1.998 | 1.7742 | 1.0764 | 1.9392 | -12.61 | -64.83 | 80.16 |
| 13.5 | | Combination dead load + Cooper's E20 | 5.952 | 5.7547 | 5.4747 | 6.0987 | -3.43 | -5.11 | 11.40 |
| 14.1 | Mid-span bending moment (kip-ft) | Dead load | 0.275 | 0.2501 | 0.2709 | 0.5464 | -10.08 | 7.68 | 101.70 |
| 14.2 | PRIMARY BOTTOM CHORD | Concentrated load at mid-span | -6.120 | -5.8892 | -8.2746 | -5.2308 | -3.92 | 28.83 | -36.78 |
| 14.3 | MS | Live load Cooper's E20 | 1.046 | 0.9752 | 1.0879 | 4.9692 | -7.24 | 10.36 | 356.77 |
| 14.4 | 285/496 | Reduced concentrated load at mid-span | -3.652 | -3.5145 | -4.9381 | -3.1216 | -3.92 | 28.83 | -36.79 |
| 14.5 | | Combination dead load + Cooper's E20 | 1.153 | 1.0508 | 1.1669 | 5.5157 | -9.75 | 9.95 | 372.68 |
| 15.1 | Mid-span bending moment (ki-pft) | Dead load | -1.198 | -1.0185 | -0.7315 | -3.5714 | -17.66 | -39.23 | 388.23 |

Historic American Engineering Record – National Covered Bridges Recording Project – 2003 – Contoocook
 Railroad Bridge
HAER No. NH-38 – pg. 24

| | | | | | | | | | | |
|------|----------------------------------|---------------------------------------|--------|---------|---------|---------|--------|--------|--------|---|
| 15.2 | PRIMARY TOP CHORD | Concentrated load at mid-span | -3.206 | -2.7511 | -1.7342 | 1.7429 | -16.54 | -58.64 | 200.50 | - |
| 15.3 | MP | Live load Cooper's E20 | -1.611 | -1.3742 | -0.8636 | 2.6264 | -17.22 | -59.12 | 404.12 | - |
| 15.4 | 463/47 | Reduced concentrated load at mid-span | -1.913 | -1.6418 | -1.0349 | 1.0401 | -16.54 | -58.64 | 200.50 | - |
| 15.5 | | Combination dead load + Cooper's E20 | -2.809 | -2.3927 | -1.5951 | -0.6382 | -17.42 | -50.00 | -59.99 | - |
| 16.1 | Mid-span bending moment (kip-ft) | Dead load | 0.568 | 0.5368 | 0.5424 | 0.8052 | -5.85 | 1.03 | 48.45 | - |
| 16.2 | PRIMARY TOP CHORD | Concentrated load at mid-span | 0.604 | 0.4273 | 0.6042 | 1.4801 | -41.40 | 29.28 | 144.97 | - |
| 16.3 | MS | Live load Cooper's E20 | 0.330 | 0.2862 | 0.3041 | 0.9564 | -15.37 | 5.89 | 214.50 | - |
| 16.4 | 253/518 | Reduced concentrated load at mid-span | 0.361 | 0.255 | 0.2796 | 0.8833 | -41.41 | 8.80 | 215.92 | - |
| 16.5 | | Combination dead load + Cooper's E20 | 0.898 | 0.823 | 0.8465 | 1.7574 | -9.16 | 2.78 | 107.61 | - |
| 17.1 | Minimum bending moment (kip-ft) | Dead load | -1.115 | -0.7874 | -0.7185 | -0.6494 | -41.66 | -9.59 | -9.62 | - |
| 17.2 | SECONDARY BOTTOM CHORD | Concentrated load at mid-span | -3.895 | -2.9782 | -2.72 | -1.3043 | -30.79 | -9.49 | -52.05 | - |
| 17.3 | MP | Live load Cooper's E20 | -2.705 | -2.0635 | -1.8603 | -1.8157 | -31.09 | -10.92 | -2.40 | - |
| 17.4 | 500/95 | Reduced concentrated load at mid-span | -2.325 | -1.7773 | -1.6232 | -0.7784 | -30.79 | -9.49 | -52.05 | - |
| 17.5 | | Combination dead load + Cooper's E20 | -3.820 | -2.8509 | -2.5789 | -2.465 | -34.01 | -10.55 | -4.42 | - |
| 18.1 | Minimum bending moment (kip-ft) | Dead load | -0.757 | -0.5218 | -0.5348 | -0.8233 | -45.11 | 2.43 | 53.95 | - |
| 18.2 | THIRD BOTTOM CHORD | Concentrated load at mid-span | -2.789 | -2.0824 | -2.1318 | -1.7162 | -33.93 | 2.32 | -19.50 | - |
| 18.3 | MP | Live load Cooper's E20 | -1.682 | -1.2735 | -1.2735 | -2.3212 | -32.06 | 0.00 | 82.27 | - |
| 18.4 | 474/97 | Reduced concentrated load at mid-span | -1.664 | -1.2427 | -1.2722 | 0.9828 | -33.93 | 2.32 | 177.25 | - |
| 18.5 | | Combination dead load + Cooper's E20 | -2.439 | -1.7688 | -1.8083 | 3.1061 | -37.89 | 2.18 | 271.77 | - |
| 19.1 | Minimum bending moment (kip-ft) | Dead load | -0.564 | -0.4112 | -0.3831 | -0.6837 | -37.14 | -7.33 | 78.47 | - |
| 19.2 | SECONDARY TOP CHORD | Concentrated load at mid-span | -2.175 | -1.72 | -1.6026 | -1.3157 | -26.44 | -7.33 | -17.90 | - |
| 19.3 | MP | Live load Cooper's E20 | -1.080 | -0.8578 | -0.8008 | -1.8159 | -25.93 | -7.12 | 126.76 | - |
| 19.4 | 498/93 | Reduced concentrated load at mid-span | -1.298 | -1.0264 | -0.9564 | -0.7852 | -26.44 | -7.32 | -17.90 | - |
| 19.5 | | Combination dead load + Cooper's E20 | -1.644 | -1.269 | -1.1839 | -2.4996 | -29.56 | -7.19 | 111.13 | - |
| 20.1 | Minimum bending moment (kip-ft) | dead load | -0.349 | -0.3659 | -0.3708 | 0.5519 | 4.76 | 1.32 | 248.84 | - |
| 20.2 | LATTICE MEMBERS | concentrated load at mid span | -1.245 | -1.4036 | -1.4219 | 0.9923 | 11.27 | 1.29 | 169.79 | - |
| 20.3 | MP | Live load Cooper's E20 | -0.770 | -0.8781 | -0.8928 | 1.5534 | 12.37 | 1.65 | 273.99 | - |
| 20.4 | 455/79 | reduced concentrated | -0.743 | -0.8376 | -0.8485 | 0.5922 | 11.27 | 1.28 | 169.79 | - |
| 20.5 | | Combination dead load + Cooper's E20 | -1.118 | -1.244 | -1.2635 | 2.1054 | 10.13 | 1.54 | 266.63 | - |

These data suggested the following observations and conclusions:

The maximum tension was in the upper primary chord, above the central pier (Figure 22). It was 1.98 times greater than the maximum value in the lower primary chord, under dead load condition. (The perfect beam behavior for uniformly distributed load produced a 1.77 ratio for bending moments). Under the mid-span concentrated load, the ratio was 1.33 for the concentrated force (compared to 1.2 for the perfect beam behavior's bending moment ratio).

The axial force distribution data showed that the overall behavior was closer to a self-formed arch with tension tie than to a continuous girder (Figure 22). The same conclusion could also be derived by comparing maximum tension values in the lower primary chord to compression values in the upper primary chords. These were not equal, as equivalent beam theory would suggest.

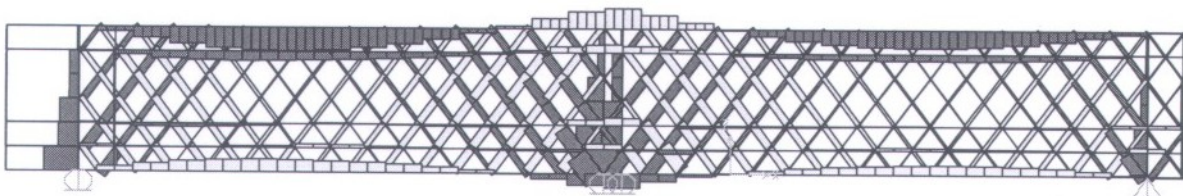


Figure 22. Axial force diagram at Combination 1, dead load + Cooper's E20

The maximum tension in the primary upper chord was more influenced by the lack of continuity in the lower chord than the overall stiffness; 8.65 percent in comparison to 7.73 percent versus control.

The same compression diagram that is specific to the overall behavior of the Town lattice truss (compression arch line) repeated locally for the secondary and tertiary lower chords. In the presence of a large concentrated force, the adjacent chord members became compressed.

The maximum tension in secondary lower chord above the pier represented 46 to 48 percent of the maximum mid-span tension in the primary chord (Figure 23). The mid-span value of L-2 was only 28 to 38 percent of that of L-1. The efficiency of secondary lower chord above the pier was reduced significantly (11.82 - 20.31 percent) due to the lack of continuity in the lower chord elements. The introduction of pins at the lattice ends had no major influences, except on tension in the secondary lower chord at the pier, which was reduced 13.78 percent. The axial forces of Cooper's E20 did not perturb the overall beam behavior of the secondary lower chord.

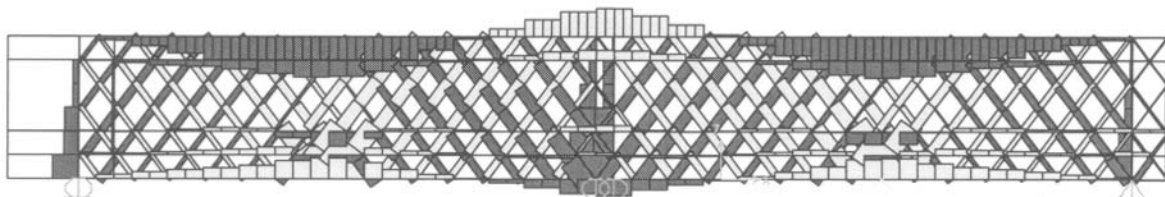


Figure 23. Axial force diagram at Load 2, mid-span concentrated force

The tertiary chord was strongly compressed for a large, local concentrated load in mid span region. For dead and Cooper's E20 live load, there was very little tension at mid span, only

0.072 kip. The tertiary lower chord was efficient above the pier, although its efficiency was reduced significantly (14.25 percent) due to the discontinuity of the chords. At quarter points the tertiary lower chord was under minor compression, both for dead and Cooper’s E20 live load.

The maximum axial force in the primary upper chord was at mid span for live loads and the combination of dead plus E20 loads. The only load condition that caused more tension above the pier in the primary upper chord than the absolute value of the mid span compression was dead load alone.

As the data in Table 9 showed, lattice members became less efficient when the span was doubled and the middle support removed. In that case, the mid-span deflection increased 1,446 percent, the maximum tension in primary lower chord increased 589 percent, and the maximum compression in primary upper chord increased 460 percent. The tension in lattice members over the pier increased only 41 percent, while compression at the middle pier increased 109 percent.

Table 9. Increase of axial force for single-span versus two-span continuous truss

| Load case | Single- span / double- span tension diagonal | Single-span / double-span compression diagonal |
|---------------------------------------|----------------------------------------------|------------------------------------------------|
| Dead load | 2.34 | 2.45 |
| Concentrated load at mid-span | 1.40 | 1.32 |
| Live load Cooper's E20 | 2.41 | 3.11 |
| Reduced concentrated load at mid-span | 1.40 | 1.32 |
| Combination dead load + Cooper's E20 | 2.39 | 2.87 |

Doubling the span increased the tension in inclined diagonals at abutments between dead load and Cooper’s E20 conditions by 2.34 to 2.41 times, and compression in declined diagonals at abutments between 2.45 and 3.11 times.

The efficiency of tension and compression lattice webs placed at mid-span (MS) versus those placed over the supports (abutments and middle pier) can be seen on the Table 10.

Table 10. Efficiency of mid-span lattice webs

| Load case | Double-span tension in MP/MS lattice % | Single-span tension in MP/MS lattice % | Double-spans compression in MP/MS lattice % | Single-spans compression in MP/MS lattice % |
|--------------------------------|----------------------------------------|----------------------------------------|---------------------------------------------|---------------------------------------------|
| Dead load | 31.68 | 8.81 | 3.79 | -0.24 |
| Concentrated load at mid- span | 365.00 | 523.19 | 70.54 | 60.05 |
| Live load Cooper's E20 | 30.64 | 30.73 | -7.69 | -8.84 |

| | | | | |
|---------------------------------------|--------|--------|-------|-------|
| Reduced concentrated load at mid-span | 364.98 | 523.21 | 70.54 | 60.05 |
| Combination dead load + Cooper's E20 | 30.88 | 24.62 | -4.37 | -6.25 |

For shorter spans, tension members at mid-span were still approximately 30 percent efficient for dead load. Tension members remained similarly efficient for Cooper’s E20 (30.64 - 30.73 percent).

Compression diagonals at mid-span were almost useless for dead loads, and locally could become tension members depending on the relative position of live loads. Even the secondary compression effect from an “out of scale” concentrated load was reduced by 70 percent (60 percent for the single span).

Lattice members were less influenced (3 percent) by reductions in chord members’ sectional areas due to splices, except in the presence of a concentrated load, where it could increase by as much as 20 percent.

Table 11 is a comparison of bending moments for the two-span bridge.

Table 11. Bending moment comparison

| Load case | Bending moment above support kip-ft | ratio to mid span |
|---------------------------------------|-------------------------------------|-------------------|
| Dead load | -2.58 | 3.51 |
| Concentrated load at mid- span | -8.99 | 2.68 |
| Live load Cooper's E20 | -8.72 | 1.59 |
| Reduced concentrated load at mid-span | -5.36 | 2.68 |
| Combination dead load + Cooper's E20 | -11.30 | 1.90 |

Negative bending moments for chords at abutments and the pier were not included in Table 11, as they represent several times greater value than the mid-span bending moment for the adjacent “span” between two lattice suspension points.

For the reduced chord section, the bending moment capacity is:

$$M_{cap} = S \times \sigma' = 10.827 \text{ kip-ft}$$

One interpretation of this is that no higher bending moment concentration can happen, thus causing first rotation and bending moment redistribution, rather than a collapse of extra loaded elements.²³

Figures 24 and 25 show that bending moment is not a characteristic strain for mid-span secondary and tertiary chords or lattice members. Their maximum bending moment values range between 0.0511 and 0.0846 kip-ft.

²³ Bending moment capacity calculation considered a NDS max. allowable stress 775psi reduced with 205psi pressure resulting from compression of the same chord member.

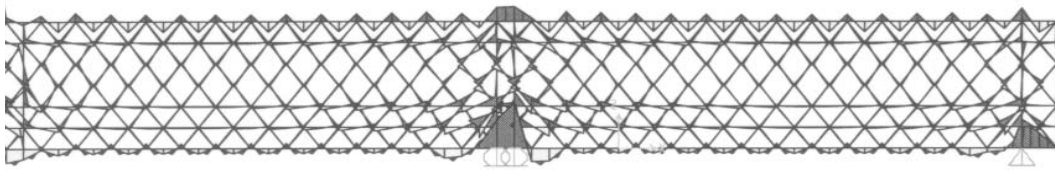


Figure 24. Bending moment diagram, Var 3, dead load

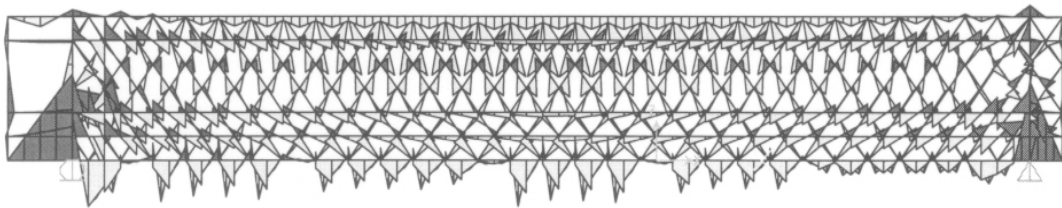


Figure 25, Bending moment diagram Var 4, dead load + Cooper's E20

Further variants, Var 5 and Var 5', were developed to model a continuous chord and no tertiary lower chord, as well as a reduced-section chord also missing the tertiary chord, to compare the efficiency of introducing tension joints to chords versus the efficiency of the tertiary chord. Table 12 presents these data.

Table 12. Comparison of efficiency of tertiary chord versus tension joints for chords

| Deflection with reduced chord without tertiary chord (in) | Deflection with full chord without tertiary chord (in) | Deflection with reduced chord with tertiary chord (in) | Decrease through tension joints (%) | Decrease though tertiary chord (%) |
|-----------------------------------------------------------|--------------------------------------------------------|--------------------------------------------------------|-------------------------------------|------------------------------------|
| 0.072429 | 0.072429 | 0.0732 | -2.33 | 1.10 |
| 0.620349 | 0.620349 | 0.5928 | -8.24 | -4.43 |
| 0.15531 | 0.15531 | 0.1543 | -7.50 | -0.68 |
| 0.370208 | 0.370208 | 0.3538 | -8.24 | -4.43 |
| 0.227739 | 0.227739 | 0.2275 | -5.86 | -0.11 |

Stiffness could be increased only 6 to 7.5 percent by introducing tension joints (according to two-dimensional modeling). From overall stiffness point of view, the tertiary chord had almost no effect, just 0.11 - 0.68 percent for live and combination loads.

Under large, "out of scale" concentrated loads, tertiary chords could have a measurable effect, but in reality, such large, concentrated forces would not be applied. Thus, J. P. Snow's opinion about the lack

of efficiency of tertiary chords was confirmed.²⁴ They should have some overall effect on the lateral stability of the web, but the models used did not consider lateral loads.

The model without studs (posts) at the middle pier showed a reduction in overall stiffness (measured in deflection at mid-span) of 27 to 30 percent.

SUBSTRUCTURES

Suspended floor system

The suspended floor system of the Contoocook Bridge was a common, historic design for double-web Town lattice bridges.²⁵ An analysis of the transmission of the maximum axle force from a floor beam to the primary lower chord was performed to determine:

- the bending and shear capacity of the floor beam.
- the perpendicular compression stress on the timber under the washers.
- the tension in the suspension rods.

Bending capacity of the floor beams

All of these floor beams have the overall length of 21 feet. The worse static situation was with suspension points at the outer lattice webs, forming a 19-foot span, as shown in Figure 26.

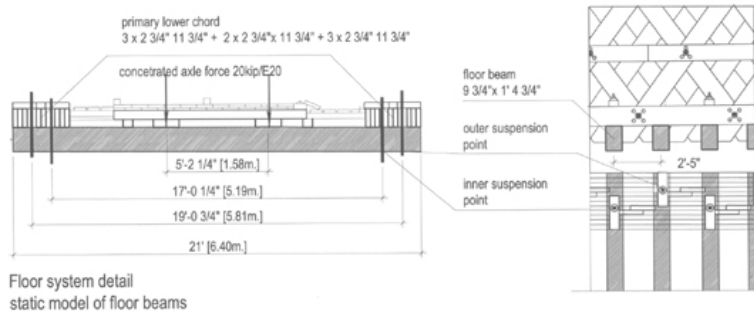


Figure 26. Floor beam detail

There were three load cases for the beam itself:

- uniform distributed load on line – self weight.
- double concentrated force from stringers, rail beam, and ties.
- Double-axle force as a live load

Flexure stress is the sum of flexure stresses due to the above mentioned load conditions:

$$\sigma = \sigma_1 + \sigma_2 + \sigma_3$$

Floor beams were not tested to identify the timber, but historic sources commonly cite yellow pine in this application, so yellow pine was assumed to be the material used here.²⁶ The allowable stresses are as follows:²⁷

| Species and commercial grade | Bending F_b (psi) | Tension II grain, F_t (psi) | Shear II grain, F_v (psi) | Compression \perp grain, $F_{c\perp}$ (psi) | Compression II grain, F_{cII} (psi) | Modulus of elasticity, E |
|--------------------------------------------------------|---------------------|-------------------------------|-----------------------------|-----------------------------------------------|---------------------------------------|----------------------------|
| Spruce, pine, & fir Select structural 5" x 5" & larger | 858 | 507 | 122.5 | 310.25 | 604.5 | 1066000 |

²⁴ J., P. Snow, "Wooden Bridge Construction on the Boston and Maine Railroad", 1895., 31-43.

²⁵ J., P. Snow, "Wooden Bridge Construction on the Boston and Maine Railroad", 1895., 31-43.

²⁶ J., P. Snow, "Wooden Bridge Construction on the Boston and Maine Railroad", 1895., 31-43.

²⁷ American Forest & Paper Association, American Wood Council, "Design Values for Wood Construction", *Supplement National Design Specification*, 2001, table 4D, 47.

Note: As it is historic 19th century timber, this was considered to be the best quality from actual NDS design values.

The analytical results are shown in Table 13.

Table 13. Bending and stress in floor beams

| No. | Version description | <i>P</i> | <i>w</i> | <i>l</i> | <i>x</i> | <i>b</i> | <i>c</i> | <i>R</i> | <i>Mmax</i> |
|-----|--------------------------------------------------------------|----------|----------|----------|----------|----------|----------|----------|-------------|
| | | kip | plf | ft | ft | ft | ft | kip | pft |
| 1 | Bending moment from self weight - outer suspension | | 31.25 | 21.00 | 7.00 | 19.00 | 1.00 | 0.33 | 1394.53 |
| 1' | Bending moment from self weight - inner suspension | | 31.25 | 21.00 | 7.00 | 17.00 | 2.00 | 0.33 | 1066.41 |
| 2 | Bending moment from dead load on stringer - outer suspension | 0.3 | | 19.00 | 7.00 | | | 0.27 | 1620.00 |
| 2' | Bending moment from dead load on stringer - outer suspension | 0.3 | | 17.00 | 7.00 | | | 0.27 | 1350.00 |

$w = 31.25 \text{ pfl (dead load)}$

| width in | depth in | <i>A</i> in ² | <i>W</i> in ³ | σ_1 psi | σ_2 | <i>Fb</i> psi | σ_3 psi |
|-------------|-------------|-----------------------------|-----------------------------|-------------------|------------|------------------|-------------------|
| 9.75 | 15.75 | 153.56 | 403.10 | 41.51404 | | 858 | |
| 9.75 | 15.75 | 153.56 | 403.10 | 31.74603 | | 858 | 768.2599 |
| 9.75 | 15.75 | 153.56 | 403.10 | | 48.22606 | 858 | |
| 9.75 | 15.75 | 153.56 | 403.10 | | 40.18838 | 858 | 786.0656 |

- σ_1 = stress from uniform load along line (self weight)
- σ_2 = stress from dead load through stringer
- Fb* = allowable stress from bending
- σ_3 = allowable stress from bending from live load (axle)

The maximum half-axle force for the inner and outer suspended floor beams are:

$$P_1 = 3.66 \text{ kip (NDS value)}$$

$$P_2 = 4.38 \text{ kip (NDS value)}$$

Working with Snow’s 1200 psi allowable stress the values are:

$$P_1^s = 5.13 \text{ kip (Snow’s value)}$$

$$P_2^s = 6.12 \text{ kip (Snow’s value)}$$

Note: these are the limit values that one single beam can carry.

The first two members of the flexure stress are known, so the third component can be calculated when the sum itself is equal to the allowable stress. Two sets of calculations have been carried out, one using the NDS allowable stresses, and one, termed “Snow’s value,” using historic allowable stress values published by him.

The maximum half-axle force for the inner and outer suspended floor beams are:

$$P_1 = 3.66 \text{ kip (NDS value)} \qquad P_1^s = 5.13 \text{ kip (Snow’s value), full axle 11.25 kip}$$

$$P_2 = 4.38 \text{ kip (NDS value)} \qquad P_2^s = 6.12 \text{ kip (Snow’s value)}$$

Maximum tension in suspension rods

Table 14 lists the maximum allowable tensions corresponding to a 20,000-psi allowable stress for the two rod sizes used in the bridge.

Table 14. Maximum tension in suspension rod

| Name | <i>D</i> in | <i>A</i> in ² | Allowable stress psi | <i>Ft</i> kip |
|---------------------------------|----------------|-----------------------------|-------------------------|------------------|
| Suspension rod tension capacity | 1.5 | 1.77 | 20000 | 35.325 |
| Suspension rod tension capacity | 1.25 | 1.23 | 20000 | 24.5313 |

$P_{sr} = 24.53 \text{ kip}$, so even with a 50-percent reduction of working area, the allowable stress was a much larger value than the one given by flexure of the floor beams. (Snow used an allowable stress of 10,000 psi for wrought iron, reducing the capacity *Ft* to 12.26 kip.)

Maximum compression perpendicular to grain

Table 15 shows the maximum compression perpendicular to the grain of the wood generated by the suspender rods through both circular and square washers.

Table 15. Maximum compression perpendicular to grain

| Name | <i>D</i> in | <i>A</i> in ² | <i>F_{cp}</i> psi | <i>F_{cp}</i> psi | <i>P_{cp}</i> kip | <i>P_{cp}</i> kip | <i>P_{cp}^s</i> kip |
|----------------------------------------------------------|----------------|-----------------------------|------------------------------|------------------------------|------------------------------|------------------------------|------------------------------------------|
| Compression perpendicular on grain under circular washer | 5.50 | 23.75 | 310.25 | 360.00 | 7.37 | 6.77 | 7.95 |
| Compression perpendicular on grain under square washer | 6.00 | 36.00 | 310.25 | 360.00 | 11.17 | 10.57 | 12.36 |

$P_{cp} = 6.77$ kip (NDS value)

$P_{cp}^s = 7.95$ kip (Snow's value)

These analyses of substructure components and systems suggested that, for Cooper's E20 load capability (a maximum axle load of 20 kip), the floor system had to be stiff enough in the longitudinal direction to share loads between at least two adjacent beams.

Comparison of three-dimensional finite element models

Three-dimensional models were constructed to allow a comparison with the two-dimensional model. The same finite element analysis software (SAP2000) was used for both models.

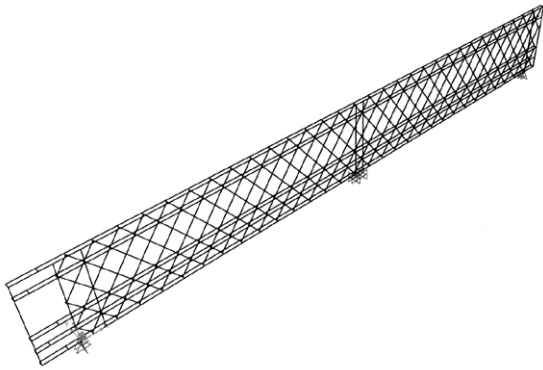


Figure 27. Axonometric view of the inner lattice truss, three-dimensional model

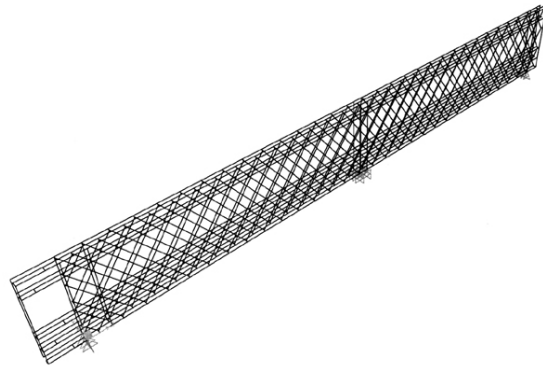


Figure 28. Axonometric view of the double lattice truss, three-dimensional model

Overall stiffness of the structure, three- versus two-dimensional models

Referenced to the equivalent beam model, the overall behavior of the structure was similar for both models. The distribution of axial forces, shear forces and bending moments were similar as well, but the overall stiffness calculated differed remarkably. Table 16 shows deflections (inches at mid-span) calculated by the following models:

- 2D inner lattice truss
- 2D total (double truss)
- 3D inner lattice truss
- 3D integral – double lattice truss

Table 16. Deflections calculated by two- and three-dimensional models

| No. | Load condition | 2D Inner | 2D Total | 3D Inner | 3D Integral |
|-----|---------------------------------------------|----------|----------|-----------|-------------|
| 1 | Dead load | -0.0727 | -0.04835 | -0.106515 | -0.100171 |
| 2 | Live load Cooper's E20 | -0.20533 | -0.10233 | -0.325431 | -0.26034 |
| 3 | Reduced concentrated load at mid-span | -0.32219 | -0.1831 | -0.64902 | -0.497939 |
| 4 | Combination dead load + Cooper's E20 | -0.27803 | -0.15067 | -0.431946 | -0.360511 |

Using the results of the above table the following conclusions were suggested concerning the efficiency of doubling the truss:

Under dead load condition, the double lattice webs deformed almost as much as the single ones. They were connected only through the middle planks of the chords and actually deformed almost independently.

A two-dimensional model for a double lattice structure would significantly mislead interpretation of stiffness. As the data in Table 16 show, deflections calculated by the three-dimensional model are 2 to 2.5 times greater than the ones from a two-dimensional model, due to it being over-stiffened by the high number of infinite stiff joints that do not exist in the reality.

Reflecting on the equivalent beam analysis, which did not take into consideration any rotation or deformation that is possible (even in a 2D model with infinite stiff inner lattice joints) the equivalent beam deflection was 56 percent less than the two-dimensional model predicted. For a single Town lattice truss, the two-dimensional analysis calculated deflections 50 percent less than those generated by the three-dimensional model, so the actual stiffness was one-half of that suggested by the equivalent beam analysis. The differences were even larger (four times) for double lattice trusses

Characteristic element forces in the three-dimensional models

Table 17 synthesizes the member forces on a lower chord member, a compression lattice member, and a tension lattice member, all at the middle pier, comparing the single-truss, three-dimensional model (white background) to the double-truss, three-dimensional model (shaded background).

Table 17. Principal forces in typical elements

(a) Tension lattice member

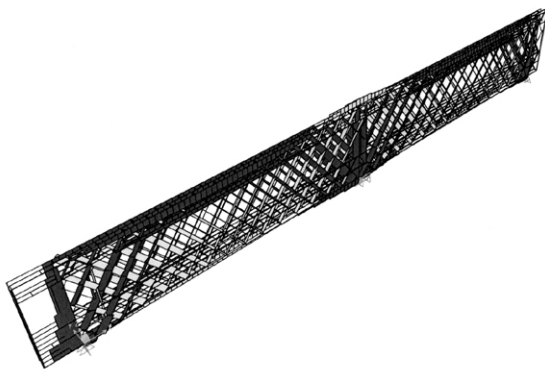
| Frame | Load | P | P | V2 | V2 | V3 | V3 | T | T | M2 | M2 | M3 | M3 |
|-------|--------------|-------|-------|----------|-----------|----------|-----------|--------|---------|--------|--------|--------|--------|
| | | kip | kip | kip | kip | kip | kip | kip-ft | kip-ft | kip-ft | kip-ft | kip-ft | kip-ft |
| 906 | Dead | 2.573 | 2.18 | 0.002373 | -0.006314 | 0.007135 | -0.003121 | 0.0404 | 0.0236 | 0.0081 | 0.0023 | 0.0114 | 0.0347 |
| 906 | E20 | 7.043 | 4.376 | -0.077 | -0.062 | 0.017 | 0.007062 | 0.0887 | -0.045 | 0.0178 | -0.082 | 0.157 | 0.0939 |
| 906 | Concentrated | 5.94 | 2.695 | 0.004821 | -0.012 | 0.035 | -0.002634 | 0.1378 | 0.0256 | 0.015 | -0.016 | 0.0079 | 0.0015 |
| 906 | Combination | 9.616 | 6.556 | -0.075 | -0.068 | 0.024 | 0.003941 | 0.1291 | -0.0214 | 0.0259 | -0.08 | 0.1684 | 0.1287 |

(b) Compression lattice member

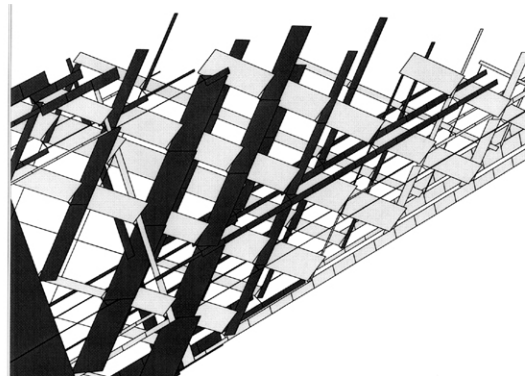
| Frame | Load | P | P | V2 | V2 | V3 | V3 | T | T | M2 | M2 | M3 | M3 |
|-------|--------------|---------|---------|--------|--------|-------|-------|--------|--------|--------|--------|---------|---------|
| | | kip | kip | kip | kip | kip | kip | kip-ft | kip-ft | kip-ft | kip-ft | kip-ft | kip-ft |
| 1058 | Dead | -7.04 | -6.582 | -0.135 | -0.119 | 0.057 | 0.053 | 0.0572 | 0.0457 | 0.2234 | 0.199 | -0.3403 | -0.3085 |
| 1058 | E20 | -17.963 | -10.874 | -0.341 | -0.21 | 0.151 | 0.106 | 0.1235 | 0.0423 | 0.5732 | 0.3444 | -0.8994 | -0.566 |
| 1058 | Concentrated | -16.983 | -9.101 | -0.258 | -0.127 | 0.144 | 0.072 | 0.1447 | 0.0702 | 0.5576 | 0.272 | -0.7215 | -0.3734 |
| 1058 | Combination | -25.003 | -17.457 | -0.476 | -0.329 | 0.208 | 0.16 | 0.1807 | 0.088 | 0.7966 | 0.5434 | -1.2397 | -0.8746 |

(c) Primary lower chord member

| Frame | Load | P | P | V2 | V2 | V3 | V3 | T | T | M2 | M2 | M3 | M3 |
|-------|--------------|---------|---------|-------|-------|--------|--------|--------|---------|--------|--------|----------|----------|
| | | kip | kip | kip | kip | kip | kip | kip-ft | kip-ft | kip-ft | kip-ft | kip-ft | kip-ft |
| 1033 | Dead | -3.204 | -3.351 | 1.301 | 1.256 | -0.124 | -0.103 | 0.142 | -0.0122 | 0.4705 | 0.307 | -3.8986 | -3.7492 |
| 1033 | E20 | -11.488 | -7.186 | 4.613 | 4.043 | -0.335 | 0.037 | -0.538 | -2.0919 | 1.2702 | -0.957 | -13.5046 | -11.4431 |
| 1033 | Concentrated | -12.651 | -8.841 | 2.008 | 1.185 | -0.333 | -0.143 | 0.5079 | -0.7606 | 1.41 | 0.445 | -7.808 | -4.7106 |
| 1033 | Combination | -14.693 | -10.537 | 5.914 | 5.299 | -0.459 | -0.066 | -0.396 | -2.1041 | 1.7406 | -0.65 | -17.4032 | -15.1923 |



(a) General distribution



(b) Detailed distribution

Figure 29. Axial force distribution

These results suggested the following conclusions:

Axial forces were reduced 50 to 60 percent for live load in all analyzed members by introducing the second lattice. With dead load more equally and directly loading the members, the reduction in that case was limited to 5 - 18 percent.

Vertical shear forces (V2) were not shared much between lattice webs as axial force distribution. They were reduced only 10 percent for chord members (where they were considerable forces), but for lattice members shear is negligible.

Horizontal shear forces (V3) can be negligible in complete trusses, but they had measurable values for single-plank lattice trusses.

Though torsion became important when live loads were applied to floor beams hung from the inner lattice only, in reality there was already a load distribution on the floor beams that would reduce torsions significantly;

Bending around the weak axis became measurable in the three-dimensional models, but it was significantly reduced when the second lattice web was introduced;

Dead load resulted in axial force concentration in the middle chord members, as all floor beams were suspended from the middle chord planks.

CONCLUSIONS – STRENGTHS AND WEAKNESSES OF DOUBLE-WEB TOWN LATTICE TRUSS

Structural finite element analyses, using two- and three-dimensional models, revealed that the two trusses, though connected to each other, interacted less than expected, due to the limited rotational and shear stiffness of the treenail groups. The overall stiffness of the double-web Town lattice truss was only 15 to 20 percent greater than the single-web truss. In terms of mid-span deflection, the trusses acted almost independently under dead load, with stiffness only 6 percent for the double-web structure. The great stiffness of Town lattice trusses is achieved by the high number of chord-lattice and lattice-lattice joints that can transmit all of the characteristic member forces through treenail-group rotation and shear. Overall stiffness is as much due to the finite stiffness of the structural joints as to the displacement of main elements such as primary and secondary chords.

Equivalent girder theory could be as misleading, especially for short-span, extremely stiff structures like the Contoocook Bridge, as a two-dimensional model based on infinitely stiff joints. Though the two-dimensional models identified characteristic member forces well, they over-estimated overall stiffness.

Chords in Town lattice trusses consist of several planks butted together. These splices reduced the overall stiffness, but the results from the various techniques used varied widely, from about 7 – 8 percent in the two-dimensional model, to 25 percent in the three-dimensional model, and as much as 50 percent by the equivalent beam method.

The three-dimensional model, as well as experimental studies, revealed that the two trusses in the double-lattice truss were working almost independently under dead load alone. The transmission of dead loads was carried out both through the rotational, but primarily the shear, capacity of the joints, and the also have a similar, determinant role under live loads. Direct rotations and translations applied on inner chord members were not measurably transmitted to middle and outer chord members.

Double-web Town lattice trusses serving railroads were well designed from an engineering point of view. Their maximum live loads were transmitted through all structural members and sub-structures involved, with basically the same safety factors throughout.

Computer software and hardware facilities have developed rapidly. Good software and hardware resources are now available to help professionals analyze and understand these structures, although the definition of correct input data can still be challenging.

BIBLIOGRAPHY

- Brock, F. B., *Truss Bridges – An Illustrated Historical Description on all Expired Patents on Truss Bridges, which under the Law are now Public Property and Free to be Used by Anyone* – American Contract Journal October 28, 1889;
- Brungaber, Robert L. and Morse-Fortier, Leonard. *Wooden Peg Tests – Their Behavior and Capacities as Used in Town Lattice Trusses*, Vermont Department of Transportation – McFarland-Johnson consultant, Philip C. Pierce, project manager, tests performed at Massachusetts Institute of Technology, 1995;
- Davies, Morgan W. *The Theory and Practice of Bridge Construction in Timber, Iron and Steel*. Macmillan and Co. Limited St. Martin’s Street, London. 1908;
- Dreicer, Gregory K. “The Long Span. Intercultural Exchange in Building Technology: Development and Industrialization of the Framed Beam in Western Europe and the United States, 1820-1870”. Ph.D. diss., Cornell University, May 1993.
- Fletcher, Robert and Snow, Jonathan Parker. “A History of the Development of Wooden Bridges”. *American Society of Civil Engineering. Paper no. 1864*, Proceedings ASCE. 1932. Vol. LVIII, pp 1455-1498, republished No.4, New York. 1976.
- Foliente, Greg C., *History of timber Construction* - Kelley, Stephen J., Loferski, Joseph, R., Salenikovich, Alexander, Stern George E., *Wood Structures. A Global Forum on the Treatment, Conservation, and Repair of Cultural Heritage*, ASTM-STP 1351, Philadelphia, 2000, p. 3-24
- Forest & Paper Association, American Wood Council. “Design Values for Wood Construction”, *Supplement National Design Specification*. 2001.
- Graton, Milton S. *The Last of the Covered Bridge Builders*, Plymouth, N.H., 1978, 1980.
- Hartog, J. P. Den. *Strength of Materials*. Dower Publications Inc., New York. 1977.
- James, J. G. “The Evolution of Wooden Bridge Trusses to 1850”. *Journal of the Institute of Wood Sciences* 9 (December 1982);
- Keenan F. J., Suddarth S., K., Nelson S.A., *Wood Trusses and Other Manufactured Structural Components – Design and Research Status, Structural Wood Research, State-of-the-Art and Reseach Need*, edited by Itani, Refik Y, Faherty Keith F., American Society of Civil Engineers, New York, 1983, p. 175-186
- Kessel, Martin H. and Augustin, Ralf. “Investigation of Wood Connections with Oak Pegs”. *Bauen mit Holz*, April 1990, translated by Matthew D. Peavy and Richard J. Schnidt.
- Kessel, Martin H. and Augustin, Ralf. “Investigation of Load Bearing Capacity of Timber Connections with Wood Pegs”. *Bauen mit Holz*, June 1994 , translated by Matthew D. Peavy and Richard J. Schnidt
- Killer, Jos. *Die Werke der Baumeister Grubenmann*. Verlag A.G. Gebr. Leeman & CO., Zürich, 1941.
- Lewandowski, Jan L., *Strategies for the Preservation of Wooden Structures* - Kelley, Stephen J., Loferski, Joseph, R., Salenikovich, Alexander, Stern George E., *Wood Structures. A Global Forum on the Treatment, Conservation, and Repair of Cultural Heritage*, ASTM-STP 1351, Philadelphia, 2000, p. 153-160
- Mead, Jr., Edgar, *Through Covered Bridges to Concord – A Recollection of the Concord and Claremont RR*, 1970;
- Middleton, William D. *Landmarks on the Iron Road*. Indiana University Press, 1999.;
- Pierce, C. Philip. *Covered Bridge Manual*. draft;
- Snow, J., P. “Wooden Bridge Construction on the Boston and Maine Railroad”. *Journal of Association of Engineering Society* XV, July 1895.

Snow, J. P., “A Recent All-wood Truss Railroad Bridge”, *The Engineering Record*. Vol. 60., No. 17. October 23., 1909.

Vose, George L. “Wooden Pins for Lattice Bridges”. *The Railroad Gazette*, May 30.. 1879.

Yeomas, David T. *The development of timber as a structural material*, Studies in the history of civil engineering Vol.8, Ashgate Variorum Ed., Brookfield, 1999, (Rotch Library TA666.D48.1999) – ISBN 0-86078-757-5

U. S. Department of the Interior, Historic American Engineering Record. HAER No. PA-478, “Structural Study of Pennsylvania Historic Bridges”, 1997. Prints and Photographs Division, Library of Congress, Washington, D.C.

U. S. Department of the Interior, Historic American Engineering Record. HAER No. OH-122, “Eldean Bridge”, 2002. Prints and Photographs Division, Library of Congress, Washington, D.C.

U. S. Department of the Interior, Historic American Engineering Record. HAER No. VT-28, “Brown Bridge”, 2002. Prints and Photographs Division, Library of Congress, Washington, D.C.

U. S. Department of the Interior, Historic American Engineering Record. HAER No. NH-35, “Wright’s Bridge”, 2002. Prints and Photographs Division, Library of Congress, Washington, D.C.

U. S. Department of the Interior, Historic American Engineering Record. HAER No. IN-103, “Pine Bluff Bridge”, 2002. Prints and Photographs Division, Library of Congress, Washington, D.C.

U. S. Department of the Interior, Historic American Engineering Record. HAER No. NH-33, “Bath-Haverhill Bridge”, 2003. Prints and Photographs Division, Library of Congress, Washington, D.C.

U. S. Department of the Interior, Historic American Engineering Record. HAER No. VT-30, “Taftsville Bridge”, 2003. Prints and Photographs Division, Library of Congress, Washington, D.C.

U. S. Department of the Interior, Historic American Engineering Record. HAER No. NH-8, “Cornish-Windsor Bridge”, 2003. Prints and Photographs Division, Library of Congress, Washington, D.C.